© 2018. Published by The Company of Biologists Ltd | Development (2018) 145, dev166678. doi:10.1242/dev.166678

RESEARCH ARTICLE

Cell wall integrity modulates *Arabidopsis thaliana* cell cycle gene expression in a cytokinin- and nitrate reductase-dependent manner

Nora Gigli-Bisceglia[1], Timo Engelsdorf[1], Miroslav Strnad[2], Lauri Vaahtera[1], Ghazanfar Abbas Khan[3], Amel Jamoune[4], Leila Alipanah[1], Ondřej Novák[2], Staffan Persson[3], Jan Hejatko[4] and Thorsten Hamann[1,*]

ABSTRACT

During plant growth and defense, cell cycle activity needs to be coordinated with cell wall integrity. Little is known about how this coordination is achieved. Here, we investigated coordination in *Arabidopsis thaliana* seedlings by studying the impact of cell wall damage (CWD, caused by cellulose biosynthesis inhibition) on cytokinin homeostasis, cell cycle gene expression and cell shape in root tips. CWD inhibited cell cycle gene expression and increased transition zone cell width in an osmosensitive manner. These results were correlated with CWD-induced, osmosensitive changes in cytokinin homeostasis. Expression of *CYTOKININ OXIDASE/DEHYDROGENASE 2* and *3* (*CKX2*, *CKX3*), which encode cytokinin-degrading enzymes, was induced by CWD and reduced by osmoticum treatment. In *nitrate reductase1 nitrate reductase2* (*nia1 nia2*) seedlings, *CKX2* and *CKX3* transcript levels were not increased and cell cycle gene expression was not repressed by CWD. Moreover, established CWD-induced responses, such as jasmonic acid, salicylic acid and lignin production, were also absent, implying a central role of *NIA1/2*-mediated processes in regulation of CWD responses. These results suggest that CWD enhances cytokinin degradation rates through a NIA1/2-mediated process, leading to attenuation of cell cycle gene expression.

KEY WORDS: Cytokinin, Cell cycle, Cell wall integrity, Cell wall signaling, Cellulose biosynthesis, Nitrate reductase

INTRODUCTION

Chemically complex cell walls surround all plant cells and are a distinctive feature of plants. These walls form a mechanical barrier during defense but are plastic during growth, cell morphogenesis and division. This is achieved by active modulation of the wall metabolism that underpins the carbohydrate-based complex wall structure, consisting mainly of cellulose, hemicelluloses, pectins, lignin and different cell wall proteins (Höfte and Voxeur, 2017). Despite a need for coordination between plant cell wall metabolism and cell division, the processes underlying this coordination are largely unknown (Gigli-Bisceglia and Hamann, 2018). In *Saccharomyces cerevisiae*, the cell wall integrity (CWI) maintenance mechanism is intricately involved in this coordination (Levin, 2011), with a dedicated checkpoint monitoring CWI and regulating cell cycle progression (Kono et al., 2016; Levin, 2011).

In plants, CWI can be impaired during growth and following exposure to abiotic and biotic stress (Bacete et al., 2018; Feng et al., 2018; Wolf, 2017). CWI-dependent responses include modifications of cellular metabolism (such as osmosensitive changes in carbohydrate metabolism and phytohormone production), growth inhibition, modification of pectic polysaccharides and deposition of lignin and callose (Engelsdorf et al., 2018; Bacete et al., 2018; Cano-Delgado et al., 2003; Ellis and Turner, 2001; Hamann et al., 2009; Hématy et al., 2007; Tsang et al., 2011; Wormit et al., 2012; Zhao and Dixon, 2014). Osmotic support (mannitol, poly-ethylene glycol or sorbitol) can suppress most responses induced by cell wall damage (CWD) in a concentration-dependent manner both in yeast and *Arabidopsis* seedlings, suggesting that they respond similarly to CWI modifications (Engelsdorf et al., 2018; Hamann, 2015; Hamann et al., 2009; Levin, 2011). This is further supported by the observation that ARABIDOPSIS HISTIDINE KINASE1 (AHK1), which is required for osmoperception and abiotic stress responses, partially complements yeast strains deficient in osmosensing (Tran et al., 2007). In addition, MID1-COMPLEMENTING ACTIVITY1 (MCA1) from *Arabidopsis* partially complements a yeast strain deficient in the plasma membrane-localized Ca^{2+}-channel protein complex MID1-CCH1, which is involved in the yeast CWI maintenance mechanism (Levin, 2011; Nakagawa et al., 2007; Paidhungat and Garrett, 1997). In *Arabidopsis*, MCA1 mediates Ca^{2+}-based signaling processes, CWI maintenance and both hypo-osmotic stress and mechanoperception (Denness et al., 2011; Furuichi et al., 2016; Yamanaka et al., 2010). Ca^{2+}-based signaling processes are required for CWI maintenance as Ca^{2+} signaling inhibitors prevent CWD-induced phytohormone [jasmonic acid (JA); salicylic acid (SA)] and lignin production in *Arabidopsis* seedlings (Denness et al., 2011). In addition to the leucine-rich repeat receptor kinases MALE DISCOVERER 1-INTERACTING RECEPTOR LIKE KINASE 2/LEUCINE-RICH REPEAT KINASE FAMILY PROTEIN INDUCED BY SALT STRESS (MIK2/LRR-KISS) and FEI2, members of the *Catharanthus roseus* receptor-like kinase1-like family (*Cr*RLK1Ls) have been implicated in CWI maintenance (Engelsdorf et al., 2018; Franck et al., 2018). THESEUS1 (THE1) is required for CWI maintenance and resistance to *Fusarium oxysporum* f. sp. *conglutinans* infection (Hématy et al., 2007; Van der Does et al., 2017), and FERONIA (FER) is required for growth regulation during

[1]Department of Biology, Høgskoleringen 5, Realfagbygget, Norwegian University of Science and Technology, 7491 Trondheim, Norway. [2]Laboratory of Growth Regulators, Centre of the Region Haná for Biotechnological and Agricultural Research, Institute of Experimental Botany of the Czech Academy of Sciences & Faculty of Science of Palacký University, Šlechtitelů 27, CZ-78371 Olomouc, Czech Republic. [3]School of Biosciences, University of Melbourne, Parkville, VIC 3010, Australia. [4]Laboratory of Molecular Plant Physiology and Functional Genomics and Proteomics of Plants CEITEC-Central European Institute of Technology Masaryk University Kamenice 5, CZ-625 00 Brno, Czech Republic.

*Author for correspondence (Thorsten.hamann@ntnu.no)

T.H., 0000-0001-8460-5151

Received 13 April 2018; Accepted 28 August 2018

Development (2018) 145, dev166678. doi:10.1242/dev.166678

salt stress (Feng et al., 2018). The CWI maintenance mechanism could be conserved as homologs for MCA1 have been identified in *Zea mays* (NOD) and *Oryza sativa* (OsMCA1) and for THE1 in *Marchantia polymorpha* (MpTHE) (Honkanen et al., 2016; Kurusu et al., 2012; Rosa et al., 2017).

Mutations in many cell wall biosynthetic genes cause growth defects, which are possibly caused by hyperactive defense signaling (Bacete et al., 2018). Dwarf phenotypes have also been associated with loss of anisotropic cell expansion due to mutations in cellulose synthase genes (CESAs), encoding proteins that synthesize cellulose during cell wall formation and cell division (Chen et al., 2018; McFarlane et al., 2014). Cellulose biosynthesis inhibitors have become routinely used tools, because they allow CWD to be induced in a tightly controlled manner (temporally and spatially), enabling targeted studies of early and late stress responses by preventing pleiotropic long-term effects (Manfield et al., 2004; Tateno et al., 2016; Wormit et al., 2012). One of the inhibitors (C17) was identified through its ability to inhibit cell division (Hu et al., 2016). Another one, isoxaben (ISX), inhibits specifically cellulose production during primary cell wall formation in elongating and dividing cells and affects subcellular localization of the cellulose synthase complexes within minutes of application (Gutierrez et al., 2009; Heim et al., 1990; Paredez et al., 2006; Watanabe et al., 2018). ISX is frequently used because of the availability of resistance-causing mutations, such as *isoxaben resistant 1* (*ixr1-1*), which represent efficient controls (Scheible et al., 2001). The *ixr1-1* mutation resides in *CELLULOSE SYNTHASE A3* (*CESA3*), encoding a subunit of the cellulose synthase complex that is active during primary cell wall formation. ISX-triggered cellulose reduction leads to changes in gene expression, loss of anisotropic cell expansion, lignin deposition, JA and SA accumulation and ultimately cell death (Cano-Delgado et al., 2003; Ellis et al., 2002; Hamann et al., 2009; Engelsdorf et al., 2018). ISX-induced responses, including accumulation of SA, JA, reactive oxygen species (ROS) and lignin, can be suppressed by diphenylene iodonium treatment (Denness et al., 2011). Diphenylene iodonium is an inhibitor of the flavin-containing enzymes implicated in ROS production; the specificity of diphenylene iodonium is concentration dependent and its precise mode of action in plants is unknown (Kärkönen and Kuchitsu, 2015).

Plant cell walls and the cell cycle undergo major changes in response to drought and osmotic stress (Skirycz et al., 2011; Tenhaken, 2014). Whereas the response to osmotic stress is mediated by an ethylene-dependent mechanism, cytokinins are involved in drought stress adaptation both as positive and negative regulators (Li et al., 2016; Nguyen et al., 2016; Nishiyama et al., 2012). Cytokinin application to plants and cell cultures induces expression changes in genes encoding cell wall-modifying proteins (expansins, laccases and pectin-modifying enzymes), suggesting that cytokinins can modify plant cell wall metabolism (Brenner et al., 2012). Although the precise mode of action of cytokinins is unknown, dirigent-like proteins could form a regulatory element (Paniagua et al., 2017). Their expression is regulated both by cytokinins and by different biotic stresses and they mediate stereo-selectivity during lignan biosynthesis. Cytokinins also regulate plant cell cycle progression (Schaller et al., 2014). They modulate transition from G2 to M phase by regulating CDKA/B and CYCB1 activity and from G1 to S phase by controlling *CYCD3;1* expression (Scofield et al., 2013). Cytokinin amounts are regulated in different ways, including through changes in nitric oxide (NO) levels (Zürcher and Müller, 2016). NO can interact directly with *trans*-zeatin (*tZ*) type cytokinins creating nitrated and nitrosylated cytokinin species, lower both NO and *tZ* levels or inhibit phosphorylation of cytokinin signaling components (Feng et al., 2013; Liu et al., 2013). Cytokinins also regulate NO levels, which control *CYCD3;1* induction, suggesting the existence of a regulatory loop between both molecules (Shen et al., 2013; Tun et al., 2008). Mutations in *NITRATE REDUCTASE 1* (*NIA1*) and *NITRATE REDUCTASE 2* (*NIA2*) that impair nitrate assimilation and NO production are genetic tools regularly used to study NO-based signaling (Chamizo-Ampudia et al., 2017; Tun et al., 2008).

Here, we combined phenotypic and genetic characterizations of CWI and cytokinin signaling components with gene expression analysis and cytokinin measurements to investigate if and how cell cycle activity in *Arabidopsis thaliana* seedlings is coordinated with CWI. The results suggest that a *NIA1*/*2*-dependent, turgor-sensitive process, controlling expression of cytokinin-degrading enzymes, is responsible for changes in certain cytokinins in response to CWD. These changes in cytokinin levels appear to attenuate cell cycle activity by reducing *CYCD3;1* expression.

RESULTS

Osmotic treatments attenuate ISX-induced root cell shape changes

To analyze regulatory processes coordinating CWI and cell cycle progression, we determined when and how cellulose biosynthesis inhibition affects *Arabidopsis thaliana* seedling root growth and root apical meristem (RAM) organization. We used an established model system in which seedlings are grown under controlled conditions in liquid culture and cellulose production is inhibited by ISX (Hamann et al., 2009; Engelsdorf et al., 2018). We confirmed ISX specificity by determining root lengths in mock- or ISX-treated Col-0 and *ixr1-1* seedlings (Fig. 1A). Mock-treated (DMSO, ISX solvent) Col-0 and *ixr1-1* seedlings exhibited similar root lengths both at the start of (t0) and after 24 h of treatment. ISX inhibited root growth nearly completely in Col-0 seedlings whereas no inhibition was detectable in *ixr1-1* seedlings, confirming ISX specificity. Osmoticum treatments (300 mM sorbitol, s300) were included because they suppress ISX-induced responses (Hamann et al., 2009; Engelsdorf et al., 2018). Seedlings were treated with DMSO, ISX, s300 or a combination of ISX and sorbitol (ISXs300) and root lengths were measured (Fig. 1B). Root growth was reduced by s300 whereas ISX treatment caused a nearly complete stop. ISXs300 treatment resulted in an intermediate (non-additive) growth phenotype.

To determine if and when treatment effects are detectable on the meristem level, we measured both RAM length and RAM cell number in seedling roots treated for 3, 6 or 9 h. ISX treatment reduced RAM length significantly after 9 h (Fig. 1C) and cell number after 3 h (Fig. 1D). Although s300 treatments had no consistent effects on RAM length, cell number was reduced after 6 h. ISXs300 treatment resulted in RAM lengths similar to mock whereas RAM cell numbers were similar to ISX. We then measured lengths and widths of individual cells in the transition zone (Fig. 1E). ISX treatments reduced cell length after 3 h. s300 treatment alone had limited effects on cell lengths, whereas ISXs300-treated seedlings exhibited pronounced effects after 6 h. S300 treatments had no detectable effects on transition zone cell width. In ISX-treated roots, cell width was increased from 3 h onwards, whereas cells subjected to ISXs300 co-treatment exhibited intermediate widths from 6 h onwards. These results suggested that ISX treatments inhibit RAM cell division, limit cell elongation and increase cell width in the transition zone. s300 co-treatment primarily reduced the ISX-induced increase in cell width but

Development (2018) 145, dev166678. doi:10.1242/dev.166678

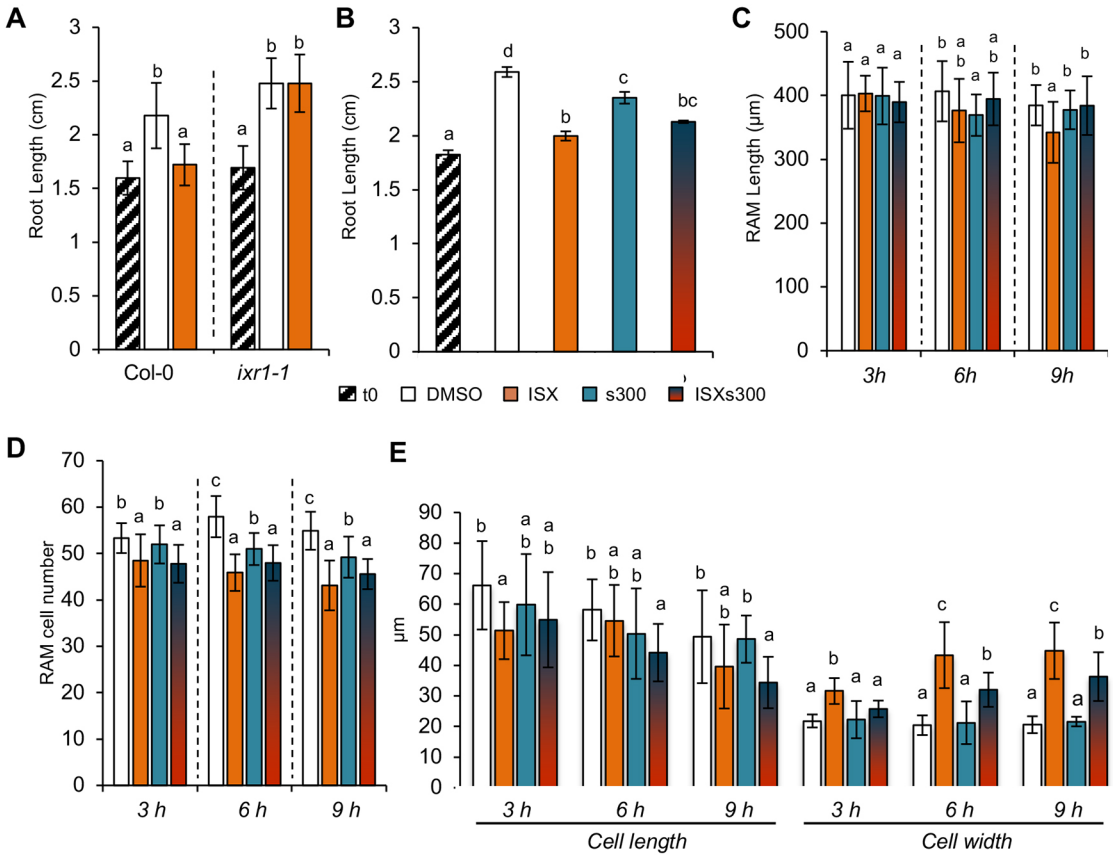

Fig. 1. ISX treatments induce sorbitol-sensitive root growth phenotypes. (A) Root lengths in Col-0 and *ixr1-1* seedlings are shown at start of (t0) and after 24 h of treatment with DMSO (mock) or isoxaben (ISX). (B) Root lengths in Col-0 seedlings at start of treatment (t0) and after 24 h of treatment with DMSO, ISX, sorbitol (s300) or ISX and sorbitol (ISXs300). (C) Seedlings were treated as in B but for 3, 6 or 9 h and RAM length was measured. (D) RAM cell number was determined for seedlings treated as in B. For A-D, *n*=25 roots were analyzed per treatment and time point. (E) Cell length and width were analyzed in the transition zone in Col-0 seedlings (*n*=10) treated as in B. Error bars represent s.d. and different letters indicate statistically significant differences according to one-way ANOVA and Tukey's HSD test (α=0.05). In A, ANOVA was used to analyze differences between the treatments in the same genotype, in B-E to analyze differences between treatments within individual time points.

effects on cell elongation were limited and no impact was detectable on ISX-induced cell division arrest.

Osmotic co-treatments attenuate ISX-triggered inhibition of cell cycle gene expression

To investigate whether ISX and osmoticum treatments affect cell cycle gene expression, we performed time course experiments with seedlings expressing a *pCYCB1;1::CYCB1;1 D-box-GUS* reporter (Colón-Carmona et al., 1999). β-Glucuronidase (GUS) staining analysis suggested that *pCYCB1;1::CYCB1;1 D-box-GUS* transcription was reduced in RAMs after 9 h of ISX treatment (Fig. 2A), whereas s300 had milder effects on reporter expression (Fig. 2A). Reporter activity in RAMs exposed to ISXs300 seemed more similar to that in s300-treated than to that in ISX-treated RAMs (Fig. 2A). This effect is not restricted to the RAM as the reporter exhibited similar expression changes also in shoot apical meristems (Fig. 2A). To obtain quantitative data, qRT-PCR-based expression analysis was performed for three genes regulating different transition steps in cell cycle progression. *CYCB1;1* regulates the G2-to-M transition, whereas *CDKB2;1* is active in the late S to M phase (Okushima et al., 2014; Schaller et al., 2014) and *CYCD3;1* is required during G1/S transition (Scofield et al., 2013). The genes examined exhibited dynamic transcript level changes with pronounced differences after 9 h (Fig. 2B). *CYCB1;1*, *CDKB2;1* and *CYCD3;1* transcript levels increased over time in mock- and s300-treated seedlings with similar dynamics (Fig. 2B). Transcript levels increased initially also in ISX-treated seedlings. However, after 3h *CYCD3;1* transcript level started to decrease whereas *CYCB1;1* plateaued and *CDKB2;1* kept increasing slightly (Fig. 2B). *CYCD3;1* and *CYCB1;1* transcript levels were significantly lower in ISX- than in mock-treated seedlings after 9 h, whereas *CDKB2;1* transcript levels did not differ between the treatments. In ISXs300-treated seedlings, transcript levels of the three genes were similar to mock controls after 9 h. To investigate whether the transcriptional effects depend on ISX-induced cellulose biosynthesis inhibition, Col-0 and *ixr1-1* seedlings were treated for 9 h and *CYCB1;1* and *CYCD3;1* transcript levels were investigated (Fig. 2C). ISX-treated *ixr1-1* seedlings exhibited no transcript changes and the changes caused by s300 were similar to Col-0. These results established that the effects of ISX are caused by cellulose biosynthesis inhibition. The qRT-PCR-based expression analysis performed so far used whole seedlings. To investigate whether the transcriptional effects are tissue specific (i.e. confined to shoot or root apical meristems), experiments were repeated and *CYCB1;1* and *CYCD3;1* transcript levels were determined in whole seedlings, shoots or roots only (Fig. S1A). Transcript levels of both genes changed in a similar manner in the different tissue types as at the whole seedling level.

We repeated the expression analysis with seedlings grown on vertically oriented plates (Fig. S1B) to investigate whether the liquid

Development (2018) 145, dev166678. doi:10.1242/dev.166678

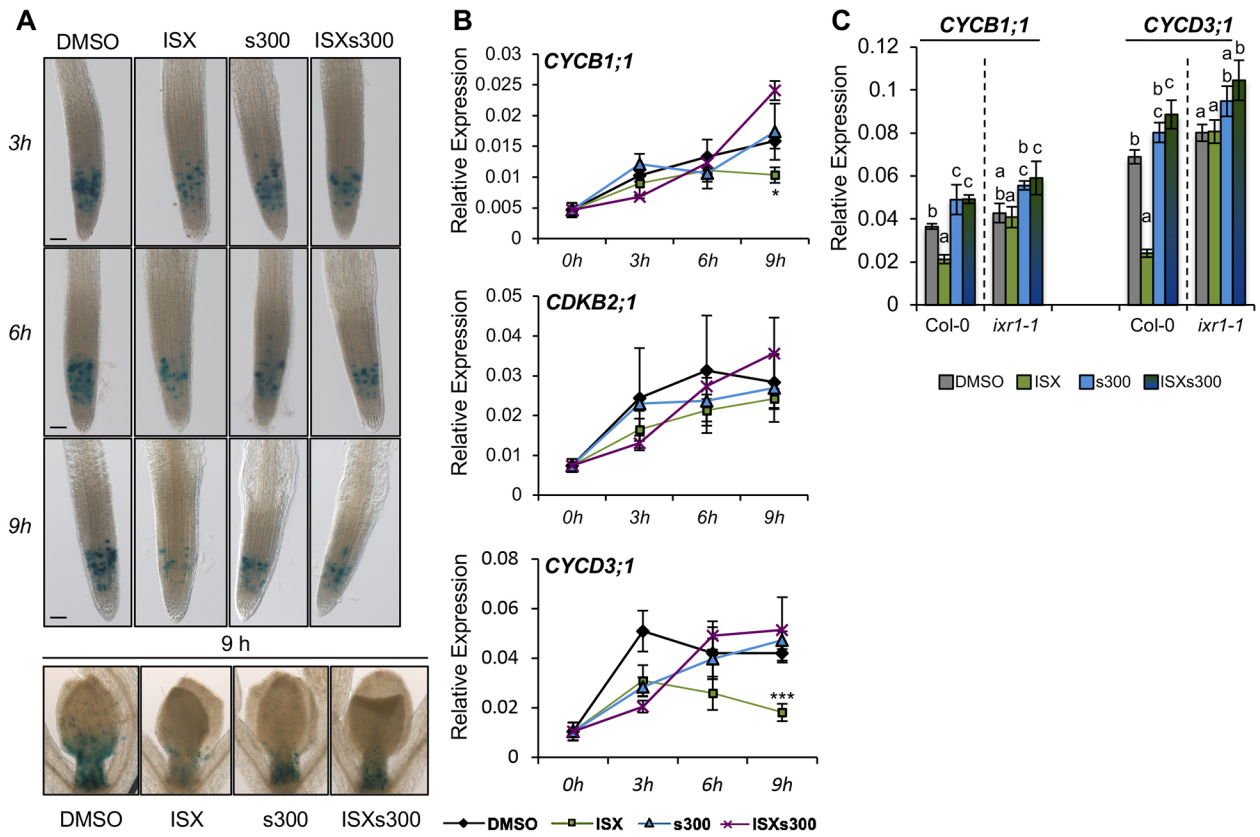

Fig. 2. ISX-induced reduction of *CYCB1;1* and *CYCD3;1* transcript levels is attenuated by sorbitol co-treatment. (A) Representative images of *pCYCB1;1::CYCB1;1:GUS* seedlings treated with DMSO, ISX, s300 or ISXs300 for different periods and stained for GUS activity (n=15). (B) Col-0 seedlings were grown and treated as in A. Transcript levels of *CYCB1;1*, *CDKB2;1* and *CYCD3;1* are shown relative to *ACTIN 2*. (C) Col-0 and *ixr1-1* seedlings were treated for 9 h as in A and gene expression analyzed as in B. Different letters denote significant differences according to one-way ANOVA and Tukey's HSD test (α=0.05) between different treatments of each genotype. Error bars represent s.d.

culture system influences the effects investigated. ISX, s300 and iSXs300 treatments had the same effects on *CYCB1;1* and *CYCD3;1* transcript levels in plate-grown seedlings as in seedlings grown in liquid culture. To investigate whether the differences in transcript levels between mock- and ISX-treated seedlings might be caused by differences in number of lateral root primordia, we quantified the number of lateral roots and lateral root primordia in mock- and ISX-treated seedlings after 6 and 12 h of treatment (Fig. S1C). No differences in the number of lateral root primordia formed were detected. These results indicate that particular growth conditions or modifications in growth dynamics are not responsible for the changes observed in the transcript levels.

ISX treatment causes displacement of CESA6 subunits from the plasma membrane (Paredez et al., 2006). We hypothesized that co-treatment with osmoticum might suppress this ISX-induced displacement, thus preventing loss of cellulose synthase activity, and tested this using a CESA6-YFP fusion protein. We determined movement speed and distribution of the fusion protein in root epidermal cells of mock-, ISX- and/or 300 mM mannitol (m300)-treated seedlings (Fig. S1D,E). m300, ISX and ISXm300 treatments all resulted in similar speed changes and displacement of CESA6-YFP fusion protein from the plasma membrane.

Transcript levels for all genes increased over time in mock-treated seedlings, possibly because fresh growth medium was added at the start of the experiments (Riou-Khamlichi et al., 2000). Differences in transcript levels became pronounced after 9 h. In ISX-treated seedlings *CDKB2;1* transcript levels did not differ significantly from mock controls, whereas *CYCB1;1* were slightly and *CYCD3;1* markedly reduced (Fig. 2C). The effects of ISX on *CYCB1;1* and *CYCD3;1* transcript levels were sensitive to osmotic manipulation to a similar extent as has been reported before for other ISX-induced responses (Hamann et al., 2009; Wormit et al., 2012; Engelsdorf et al., 2018). In all experiments *CYCD3;1* transcript levels seemed to be most sensitive to the manipulations.

ISX-induced changes in transcript levels require nitrate reductase activity

THE1 mediates certain ISX-induced CWD responses (Hamann et al., 2009; Hématy et al., 2007; Engelsdorf et al., 2018). Therefore, we investigated whether absence of *THE1*, or other genes previously implicated in CWI maintenance, affects ISX-induced reduction of *CYCD3;1* and *CYCB1;1* expression. We characterized knockouts (Kos) for *THE1*, *WALL ASSOCIATED KINASE 2* (*WAK2*), *MIK2*, *FEI2*, and the ion channels *MSCS-LIKE 2* (*MSL2*), *MSCS-LIKE3* (*MSL3*) and *MCA1* (Denness et al., 2011; Haswell et al., 2008; Hématy et al., 2007; Kohorn et al., 2006; Van der Does et al., 2017; Xu et al., 2008; Engelsdorf et al., 2018). Because JA signaling has been implicated both in CWI maintenance and regulation of *CYCB1;1*, we included a KO allele for a key JA biosynthetic enzyme (*ALLENE OXIDE SYNTHASE*, *AOS*) (Ellis and Turner, 2001; Świątek et al., 2004). To investigate a possible involvement of NO-based signaling processes, we used *nia1 nia2* seedlings. We quantified *CYCB1;1* and *CYCD3;1* transcript levels after 9 h in mock-, ISX-, s300- and ISXs300-treated seedlings. Transcript level

Development (2018) 145, dev166678. doi:10.1242/dev.166678

changes for both genes induced by the different treatments were similar in Col-0 *aos*, *mik2*, *wak2*, *fei2*, *the1* and *mca1* seedlings (Fig. S2A-C). In mock-treated *msl2 msl3* seedlings, *CYCB1;1* and *CYCD3;1* transcript levels were elevated, but relative changes in the responses were similar to Col-0 (Fig. S2D) (Wilson et al., 2016). Transcript levels in mock-treated *nia1 nia2* seedlings were similar to Col-0, but ISX, s300 and ISXs300 treatments caused no changes (Fig. 3A). To ensure that these effects were not due to indirect consequences on growth caused by changes in nitrogen metabolism in the *nia1 nia2* seedlings, we assessed seedling root growth and ISX-induced root growth inhibition in *nia1 nia2* seedlings (Fig. 3B). Root length was only slightly reduced in mock-treated *nia1 nia2* seedlings compared with Col-0 controls, and ISX treatment inhibited root growth in Col-0 and *nia1 nia2* seedlings similarly, suggesting that loss of NIA1 and NIA2 activity impairs neither growth per se nor ISX-induced root growth inhibition.

These results implicated *NIA1* and *NIA2* in CWD responses and indicated that *THE1*-mediated responses to ISX might also be nitrate

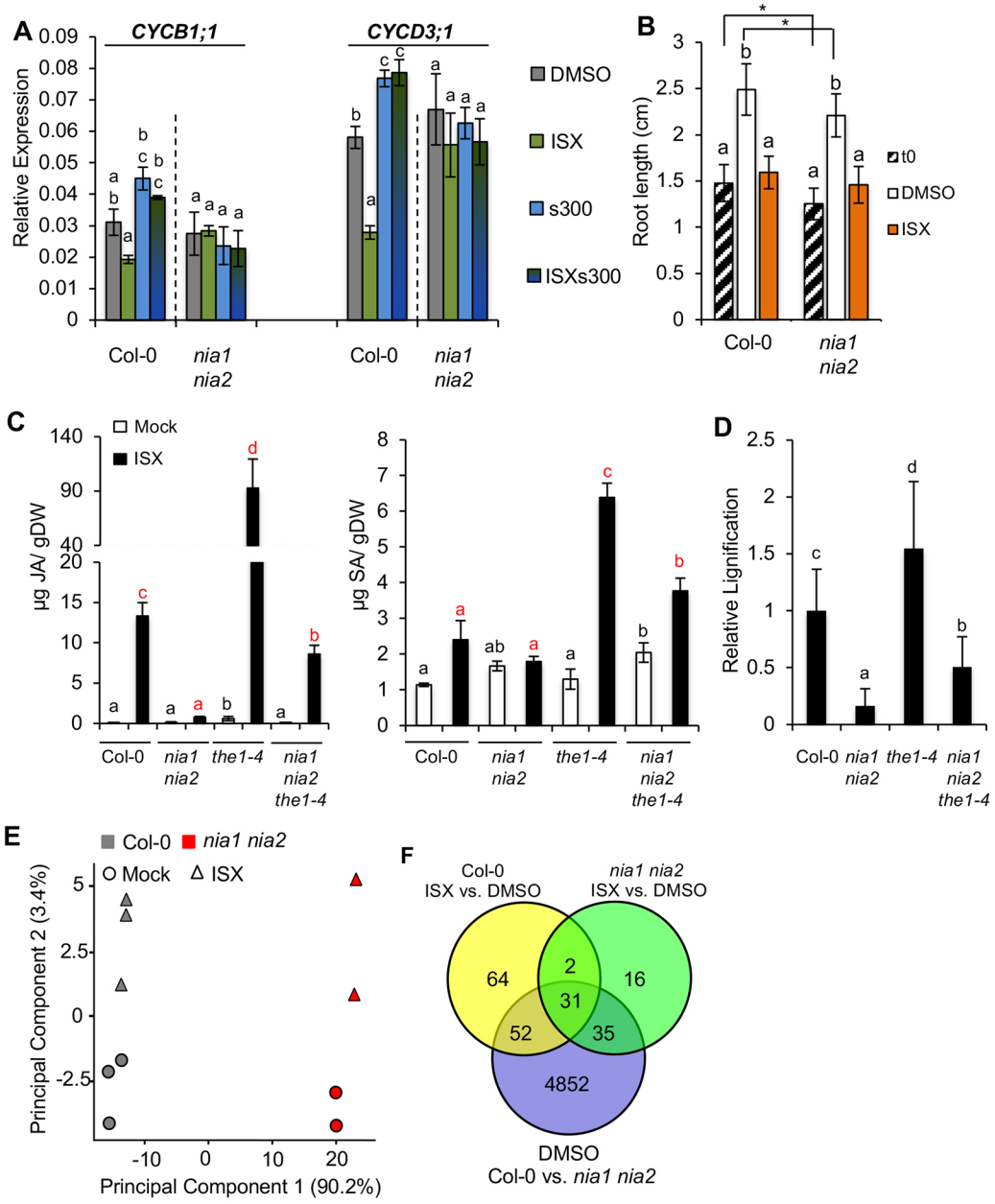

Fig. 3. ISX-activated responses are reduced in *nia1 nia2* seedlings. (A) Col-0 and *nia1 nia2* seedlings were treated for 9 h. Transcript levels of *CYCB1;1*, *CDKB2;1* and *CYCD3;1* are shown relative to *ACTIN 2*. (B) Root lengths were determined in Col-0 and *nia1 nia2* seedlings (t0) and after 24 h of treatment (n=25). (C) JA and SA accumulation were quantified in seedlings after 7 h ISX treatment. (D) Seedlings (each genotype n=20) were stained with phloroglucinol HCl after 12 h of ISX treatment to detect lignification. Quantification was performed using image analysis and is expressed relative to Col-0. (E) Principal component analysis (PCA) of next-generation sequencing (NGS) data obtained from Col-0 and *nia1 nia2* after 1 h of ISX or mock treatment (Col-0 n=3; *nia 1 nia2* n=2). (F) Venn diagram showing differentially expressed genes (P<0.01) with data deriving from the experiment shown in E. All error bars represent s.d. One-way ANOVA and Tukey's HSD test (α=0.05) were used to analyze differences in responses to treatments for each genotype and different letters denote significant differences (A,B,D). In C, results of one ANOVA performed for mock are indicated in black letters, and results of the second for ISX-treated genotypes are shown with red letters in the same figure.

Development (2018) 145, dev166678. doi:10.1242/dev.166678

reductase dependent. Therefore, we introduced a *THE1* gain-of-function allele (*the1-4*) into the *nia1 nia2* background (Merz et al., 2017). We analyzed JA, SA and lignin accumulation in Col-0, *nia1 nia2*, *the1-4* and *nia1 nia2 the1-4* seedlings after ISX treatment. In ISX-treated *nia1 nia2* seedlings, SA, JA and lignin production were dramatically reduced compared with ISX-treated Col-0 seedlings (Fig. 3C,D). Whereas ISX-induced responses were enhanced in *the1-4* seedlings compared with Col-0, responses were reduced in *nia1 nia2 the1-4* seedlings compared with *the1-4* (Fig. S3A-C). In *nia1 nia2 the1-4* seedlings, root growth was still inhibited by ISX treatment and *CYCD3;1* and *CYCB1;1* transcript levels did not respond to ISX treatment, similar to *nia1 nia2* seedlings.

To understand better the contributions of NIA1 NIA2 to ISX-induced responses, we performed an RNA-seq experiment with Col-0 and *nia1 nia2* seedlings mock- or ISX-treated for 1 h. Principal component analysis (PCA) showed that most of the differences result from the genotypes (PC1, 90.2%) whereas treatment had minor effects (PC2, 3.4%) (Fig. 3E). Gene ontology (GO) analysis of the results from mock-treated Col-0 versus *nia1 nia2* detected an over-representation of genes implicated in stress responses and primary metabolism (Table S3). Analysis of Col-0 mock versus Col-0 ISX and *nia1 nia2* mock versus *nia1 nia2* ISX showed pronounced over-representation of defense response genes (Tables S4 and S5). 4852 genes were differentially expressed between mock-treated Col-0 and *nia1 nia2* seedlings, confirming that *NIA1* and *NIA2* contribute to fundamental processes (Fig. 3F). Whereas 149 genes exhibited significant transcript-level changes in ISX-treated Col-0 seedlings versus mock, only 84 genes exhibited such changes in *nia1 nia2*. Thirty-three genes exhibited significant differences in both ISX-treated Col-0 and *nia1 nia2* seedlings compared with mock controls, suggesting that *NIA1* and *NIA2* are not required for their activation (Table S6). Among the 33 genes, several encode components of Ca^{2+}-signaling elements and ERF or WRKY family transcription factors. To confirm that the transcriptomics-derived expression data are reproducible, we selected three candidate genes (*At2g44840*, *At4g31320*, *At2g17330*) for validation by qRT-PCR-based expression analysis (Fig. S4A,B). Similar to the RNA-seq analysis-derived data, *At2g44840* expression was induced strongly in Col-0 seedlings but less so in *nia1 nia2*. *At2g17330* transcript levels were reduced in *nia1 nia2* seedlings compared with Col-0 and were not responsive to ISX. *At4g31320* transcript levels were reduced in ISX-treated Col-0 but slightly induced in *nia1 nia2* seedlings.

The transcriptomic analysis detected fundamental differences between Col-0 and *nia1 nia2*. However, results from growth assays and targeted cell cycle gene expression analysis of mock-treated seedlings detected no profound differences between *nia1 nia2* and Col-0 controls. This suggests that the effects on ISX-induced responses, detected in *nia1 nia2* seedlings, are specific. THE1-dependent CWI signaling and JA production were not required for the ISX-induced reduction of *CYCB1;1* and *CYCD3;1* transcript levels. A *NIA1/2*-dependent process seems to be required for the ISX-induced changes in *CYCB1;1* and *CYCD3;1* transcript levels and for phytohormone/lignin accumulation and also contributes to *THE1*-mediated processes.

tZ application rescues ISX-triggered transcript level changes

Cytokinins regulate cell cycle progression (Schaller et al., 2014). To investigate whether the effects of ISX on transcript levels are cytokinin dependent, Col-0 seedlings were treated for 9 h either with increasing concentrations of *tZ*, ISX alone or ISX with increasing *tZ* concentrations (Fig. 4A). *tZ* treatment alone resulted in similarly increased *CYCB1;1* transcript levels regardless of concentration. *CYCB1;1* transcript levels in seedlings co-treated with ISX and *tZ* were in between transcript levels observed in ISX- or *tZ*-treated ones. Compared with *CYCB1;1*, *CYCD3;1* transcript levels were enhanced in a concentration-dependent manner by *tZ*. Co-treatments with ISX and *tZ* led to *CYCD3;1* transcript levels similar to those of mock controls, revealing an effect of *tZ* on the ISX-induced reduction. To determine whether *NIA1* and *NIA2* are required to mediate the effects of ISX and *tZ* treatments on transcript levels, we repeated the experiments with *nia1 nia2* seedlings (Fig. 4B). In mock-treated *nia1 nia2* and Col-0 seedlings, *CYCD3;1* and *CYCB1;1* transcript levels were similar. *tZ* treatment at 100 nM or 1 µM induced elevated transcript levels for both genes whereas ISX treatment did not reduce transcript levels in *nia1 nia2* seedlings. In seedlings co-treated with ISX and 100 nM or 1 µM *tZ*, transcript levels of both genes were similar to those in seedlings treated with the corresponding *tZ* concentrations alone. These results suggested

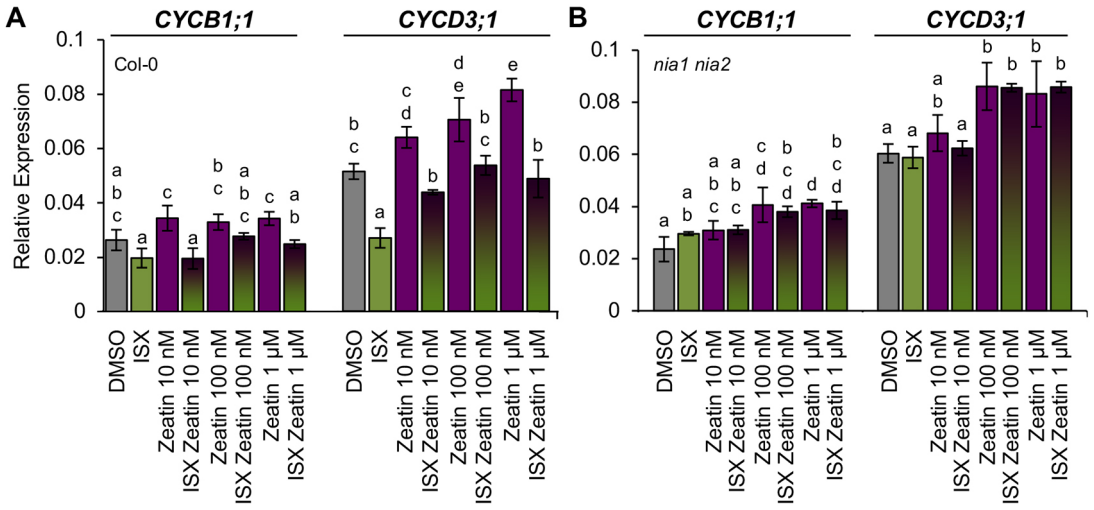

Fig. 4. ISX-induced cell cycle transcript reduction is attenuated by zeatin application. (A,B) Col-0 (A) and *nia1 nia2* (B) seedlings were treated with DMSO, ISX, DMSO/zeatin and combinations of zeatin and ISX. All error bars represent s.d. One-way ANOVA and Tukey's HSD test (α=0.05) were used to analyze the differences between treatments for each genotype and different letters denote significant differences.

Development (2018) 145, dev166678. doi:10.1242/dev.166678

that the effect of ISX on *CYCD3;1* and *CYCB1;1* transcript levels is dependent on *NIA1 NIA2* whereas the *t*Z effect is not.

Cytokinin homeostasis is changed in ISX- and osmo-treated seedlings

Results from the *t*Z experiments suggested that cytokinins modulate the effects of ISX on *CYCD3;1* and *CYCB1;1* transcript levels. To determine whether ISX treatments affect cytokinin homeostasis, we measured total cytokinins and different isoprenoid cytokinins [including *t*Z, *cis*-zeatin (*c*Z) and N^6-(Δ^2-isopentenyl) adenine (*i*P)] in Col-0 seedlings mock-, ISX-, s300- or ISXs300-treated for up to 9 h (Fig. 5). Total cytokinin and *t*Z levels increased over time in mock-treated seedlings possibly owing to increased growth caused by provision of fresh media at the start of the time course (Fig. 5). Results for the cytokinin bases *c*Z/*t*Z and *i*P suggested (mostly *c*Z-) type-specific changes after 3 h. Levels of total cytokinins and of *c*Z, *t*Z and *i*P types started to show differences after 6 h, which became pronounced after 9 h. ISX-treated seedlings exhibited reduced levels of total cytokinins and *t*Z and *i*P types whereas *c*Z types were enhanced. Sorbitol treatments resulted in intermediate levels (between ISX and mock) with the exception of total *i*P type, for which levels were similar to mock-treated controls. Intriguingly, in ISXs300-treated seedlings the levels of most cytokinin types were more similar to those of s300-treated seedlings than to ISX-treated seedlings. To investigate whether the changes might be tissue specific, we analyzed cytokinin levels in aerial parts after 9 h of treatment (Fig. S5) and found similar trends to those observed in whole seedlings.

The measurements showed that ISX treatments cause reductions in the levels of the most biologically active cytokinins (*t*Z and *i*P types),

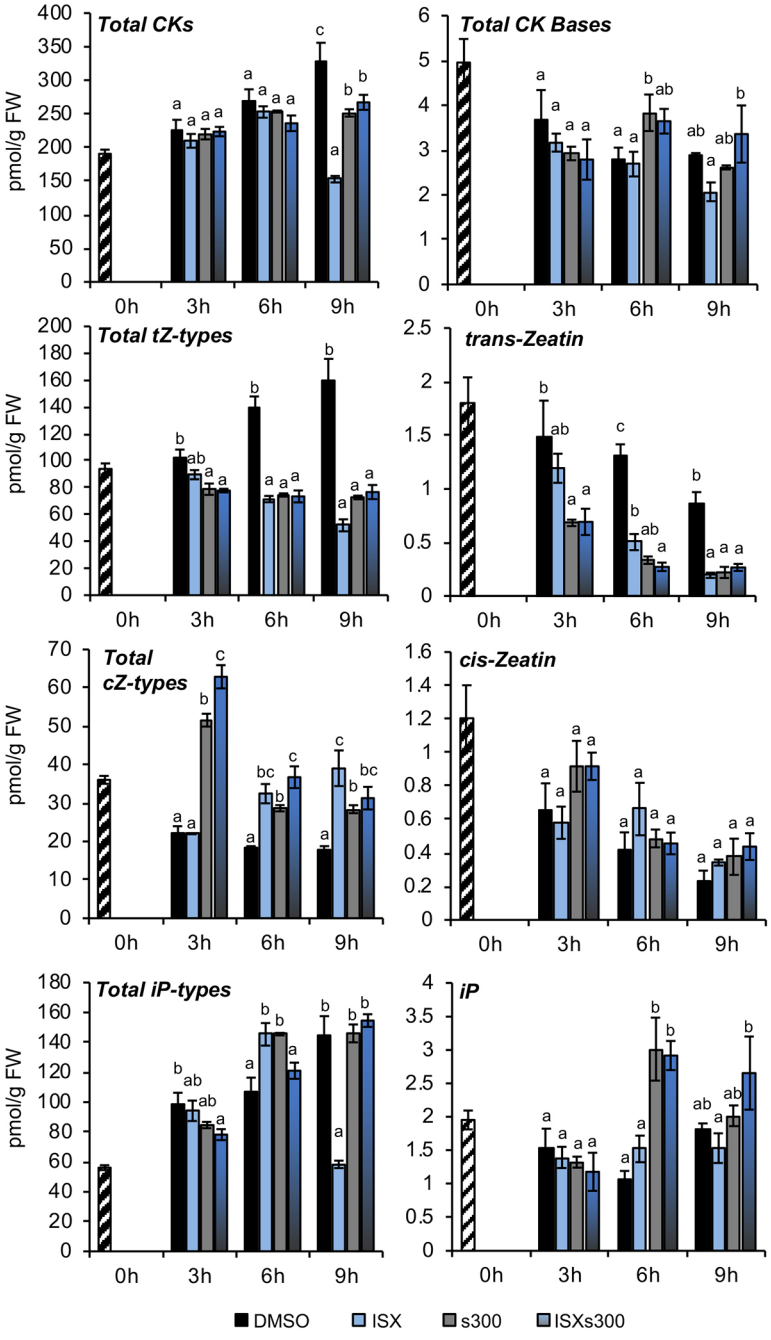

Fig. 5. Cytokinin measurements detect differential effects of ISX and osmoticum treatments. Col-0 seedlings were treated with DMSO, ISX, s300 or ISXs300. Values represent means of results from two independent experiments (n=3 each). Error bars represent s.d. One-way ANOVA and Tukey's HSD test (α=0.05) were used to analyze differences within single time points and different letters denote significant differences. CK, cytokinin.

Development (2018) 145, dev166678. doi:10.1242/dev.166678

whereas s300 treatment seemed to have the opposite effect (including the attenuation of ISX treatment effects). The changes in *i*P-type levels in ISX- and/or s300-treated seedlings appear to be closely correlated with the changes observed in *CYCD3;1* transcript levels.

CKX2 and CKX3 expression is induced in an osmo-sensitive and NIA1/2-dependent manner by ISX treatments

The results from gene expression analysis, *t*Z treatments and cytokinin profiling suggested that ISX- and osmoticum-induced effects on *CYCD3;1* and *CYCB1;1* transcript levels are mediated by a cytokinin-dependent mechanism. We therefore investigated whether cytokinin signaling is regulating the ISX- and/or osmoticum-induced effects by quantifying *CYCD3;1* and *CYCB1;1* transcript levels after 9 h in single, double and multiple KO seedlings for cytokinin perception and signaling elements including: *ARABIDOPSIS HISTIDINE KINASE 1* (*AHK1*), *AHK2*, *AHK3*, *AHK4* (also known as *CRE1*), *ARABIDOPSIS HISTIDINE-CONTAINING PHOSPHOTRANSFER PROTEIN 1* (*AHP1*), *AHP2*, *AHP3*, *AHP4*, *AHP5* and *ARABIDOPSIS RESPONSE REGULATOR 1* (*ARR1*), *ARR10*, *ARR12* (Zürcher and Müller, 2016). *CYCB1;1* and *CYCD3;1* transcript levels were reduced in mock-treated *ahk2/3*, *ahk3/4*, *ahp1/2/3/4/5* and *arr1/10/12* seedlings (Fig. S6A-D), suggesting that attenuating cytokinin signaling affects basal expression of cell cycle genes. ISX-treated *ahk1*, *ahk2/3*, *ahk3/4*, *ahk4*, *ahp1/2/3/4/5* and *arr1/10/12* seedlings showed similarly reduced transcript levels as in Col-0. *CYCB1;1* levels in s300- and ISX/s300-treated *ahk2/3* seedlings were not elevated as those induced in Col-0 by such treatments, suggesting changed sorbitol sensitivity. To investigate the possibility of genetic redundancy and growth-related defects in *AHK*-triple KO plants that might affect the responses analyzed, we repeated some of the experiments and included LGR991, an AHK4 inhibitor/AHK3 competitor (Nisler et al., 2010) (Fig. S6C). In LGR991/ISX-treated Col-0, *ahk2/3* and *ahk3/4* seedlings *CYCB1;1* and *CYCD3;1* transcript levels were still reduced. LGR991/s300-treated Col-0 seedlings exhibited lower *CYCB1;1* transcript levels than s300-treated Col-0. LGR-991 co-treated *ahk2/3* and *ahk3/4* seedlings still responded to the treatments but *CYCB1;1* transcript level changes were less pronounced in *ahk2/3*. These effects were not detectable for *CYCD3;1*.

Next, we investigated whether the effects of *t*Z treatments on *CYCB1;1* and *CYCD3;1* expression are mediated by the established cytokinin signaling mechanism (Fig. 4). Col-0, *ahk2 ahk3* and *ahk3 ahk4* seedlings were mock-, ISX-, *t*Z- or ISX/*t*Z-treated and *CYCB1;1* and *CYCD3;1* transcript levels determined (Fig. S6E). *ahk2 ahk3* seedlings exhibited lower basal transcript levels than Col-0 seedlings but responded similarly to the treatments. In ISX/*t*Z-treated *ahk3 ahk4* seedlings, *CYCD3;1* transcript levels did not recover as they did in Col-0 seedlings, suggesting that *AHK3 AHK4* are required for *t*Z perception.

Because certain cytokinins were reduced in ISX-treated seedlings, we investigated whether active degradation is responsible. Knockout of individual cytokinin oxidases (CKXs) seems to have no phenotypic effect due to redundancy (Bartrina et al., 2011). Therefore, we used overexpression lines for CYTOKININ OXIDASE 2 (*oeCKX2*, localized in the endoplasmic reticulum and apoplast) and CYTOKININ OXIDASE 3 (*oeCKX3*, residing in the vacuole) because they enabled us to test whether manipulating cytokinin levels affects *CYCB1;1* and *CYCD3;1* transcript levels and to determine whether spatial requirements may exist (Werner et al., 2003). We analyzed *CYCB1;1* and *CYCD3;1* transcript levels in *oeCKX2* and *3* seedlings. In *oeCKX2* seedlings, *CYCB1;1* transcript levels were lower in mock- and s300-treated seedlings than in Col-0 controls, whereas mock- and s300-treated *oeCKX3* seedlings were similar to Col-0 (Fig. 6A). In ISX-treated Col-0 seedlings, transcript levels were reduced whereas reductions in *oeCKX* seedlings were less pronounced. In ISXs300-treated Col-0 and *oeCKX3* seedlings, *CYCB1;1* transcript levels were similar to those of mock-treated seedlings, whereas in *oeCKX2* they were similar to those observed in ISX-treated ones. *CYCD3;1* transcript levels were reduced in mock-treated *oeCKX2* seedlings compared with Col-0. ISX-treated Col-0 seedlings exhibited reductions in *CYCD3;1* transcript levels, which were not observed in *oeCKX2* (owing to the reduction in basal expression) and less pronounced in *oeCKX3* seedlings. In s300- or ISX/s300-treated Col-0 seedlings, *CYCD3;1* levels were enhanced. In *oeCKX2* and *oeCKX3* seedlings the effects of s300 and ISX/s300 were similar to those observed in Col-0.

The impaired responsiveness of *CYCD3;1* and *CYCB1;1* in *oeCKX* lines suggested a possible role of cytokinin homeostasis/degradation in the CWD response. We performed timecourse experiments and quantified *CKX2* and *CKX3* transcript levels in Col-0 seedlings to investigate whether these effects are regulated at the transcriptional level. *CKX2* transcript levels were significantly induced in ISX-treated seedlings after 9 h (Fig. 6B). s300- and ISXs300-treated seedlings exhibited *CKX2* transcript levels similar to mock-treated controls. *CKX3* transcript levels were increased after 6 h of ISX treatment, reduced in s300-treated seedlings and similar to mock controls in ISXs300-treated seedlings. To investigate whether ISX-induced changes in *CKX2* and *CKX3* transcript levels are dependent on *NIA1* and *NIA2*, we performed timecourse experiments and investigated *CKX2* and *CKX3* transcript levels in mock- or ISX-treated Col-0 and *nia1 nia2* seedlings. Whereas *CKX2* and *CKX3* transcript levels increased over time in ISX-treated Col-0 seedlings, such increases were absent in *nia1 nia2* (Fig. 6C).

Genetic manipulation of cytokinin perception and signal translation affected osmoticum-induced changes in *CYCB1;1* transcript levels but did not affect the ISX-induced changes in *CYCB1;1* and *CYCD3;1* transcript levels. ISX-induced *CKX2* and *CKX3* expression was osmosensitive and dependent on NIA1 and NIA2 activity. Manipulating *CKX2* expression affected *CYCB1;1* and *CYCD3;1* basal transcript levels and responses to ISX and s300 treatments. These results suggest that ISX and osmoticum treatments modify *CKX2* and *CKX3* expression, which in turn seems to affect *CYCD3;1* transcript levels preferentially.

DISCUSSION

Plant cell wall metabolism and cell cycle activity are essential components of development, immunity and abiotic stress (Zhao and Dixon, 2014; Polyn et al., 2015; Zhao et al., 2017; Bacete et al., 2018). Here, we determined how CWD (impairing CWI) affects cell cycle progression and investigated the regulatory processes.

Phenotypic analysis of seedling root growth indicated that ISX-induced growth inhibition is attenuated by osmoticum (Fig. 1B). Analysis of cell number and length showed that the osmoticum effect is restricted to attenuation of RAM length, whereas RAM cell number (cell division) was still arrested (Fig. 1C,D). Cellulose is an essential element for the completion of the cross-walls separating both daughter cells after mitosis; therefore, complete inhibition of cell division is expected and is similar to effects observed in cellulose biosynthesis mutants (Chen et al., 2018; Miart et al., 2014; Nicol and Höfte, 1998). More detailed phenotypic analysis showed that ISX limits elongation in the transition zone and increases cell width in an osmosensitive manner similar to previous studies

Development (2018) 145, dev166678. doi:10.1242/dev.166678

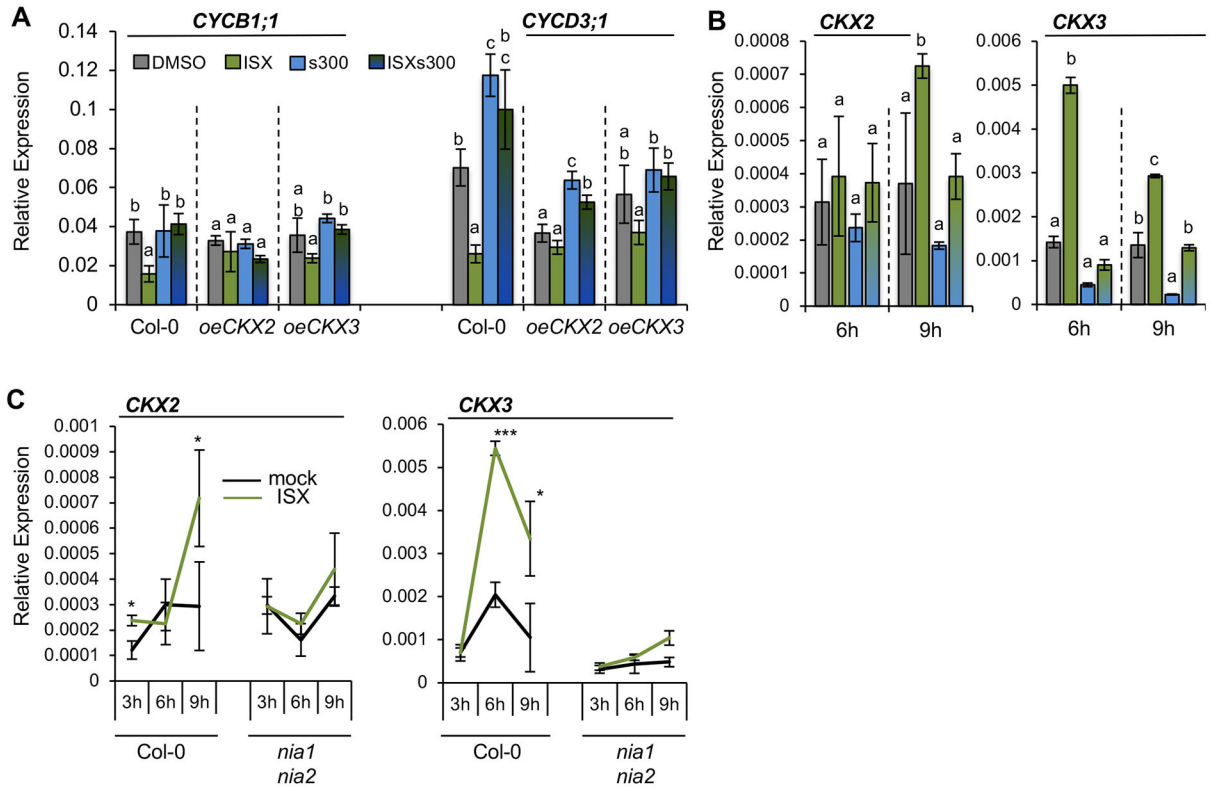

Fig. 6. *CKX2* overexpression affects ISX- and sorbitol-induced changes in *CYCD3;1* transcript levels. (A) Col-0 and *CKX2*- or *CKX3*-overexpressing seedlings (*oeCKX2*, *oeCKX3*) were treated for 9 h with DMSO, ISX, s300 or ISXs300. Transcript levels of *CYCB1;1*, and *CYCD3;1* are shown relative to *ACTIN 2*. (B) Transcript levels of *CKX2* and *CKX3* are shown in Col-0 seedlings treated as in A. (C) Col-0 and *nia1 nia2* seedlings were treated as in A and relative *CKX2* and *CKX3* transcript levels are shown. One-way ANOVA and Tukey's HSD test (α=0.05) were used to analyze the differences between treatments of each genotype (in A) or within the same time point (in B). Different letters denote significant differences. In C, pairwise comparison of ISX- and mock-treated samples was performed using Student's *t*-test. **P*<0.05, ****P*<0.001.

(Fig. 1E) (Cosgrove, 2018). Cellulose biosynthesis inhibition during cell elongation results in isodiametric cell expansion caused by the interplay of turgor pressure and weakened cell walls. Here, turgor-driven isodiametric cell expansion was apparently attenuated by addition of osmoticum. Co-treatment with osmoticum seemed to suppress primarily the ISX-induced increase of transition zone cell width but not the effects on cell division or on cell elongation, suggesting that cell shape distortion could be responsible for activation of CWD responses.

Analysis of ISX-treated *Arabidopsis* seedlings expressing the *pCYCB1;1::CYCB1;1 D-box-GUS* reporter suggested that *CYCB1;1* transcript levels are reduced by ISX and attenuated by co-treatment with osmoticum in both shoot and root apical meristems (Fig. 2A; Fig. S1). qRT-PCR-based expression analysis showed that *CDKB2;1* transcript levels did not change, suggesting that *CDKB2;1* expression is not responsive to CWD. *CYCB1;1* and *CYCD3;1* transcript levels were reduced by ISX treatment and similar to mock levels if co-treated with osmoticum. Based on the results of the phenotypic analysis, changes in transcript levels seem to occur in response to a change in cell shape and not because of cell division or elongation arrest. Similar effects of osmoticum and CWD on cell cycle and survival have been reported in yeast and other plant species (Iraki et al., 1989; Levin and Bartlett-Heubusch, 1992).

We performed a genetic analysis (including *AOS*, *MIK2*, *WAK2*, *FEI2*, *THE1*, *MCA1*, *MSL2 MSL3*) and found that genes required for ISX-induced JA/SA or lignin production are not necessary for changes in *CYCD3;1* and *CYCB1;1* transcript levels (Fig. S2). These results suggest a second pathway exists, regulating the effects on cell cycle gene expression. However, both pathways respond to an osmosensitive stimulus, indicated by the similar effects of osmoticum on ISX-induced JA, SA, lignin production and *CYCD3;1* and *CYCB1;1* transcript levels (Engelsdorf et al., 2018). As part of the genetic analysis we also examined *nia1 nia2* seedlings. Differences on the transcriptome level between Col-0 and *nia1 nia2* seedlings suggested that fundamental metabolic differences exist, in accordance with involvement of NIA1 and NIA2 in nitrogen metabolism (Fig. 3E,F) (Chamizo-Ampudia et al., 2017). However, *CYCB1;1* and *CYCD3;1* transcript levels and seedling root lengths were similar in mock-treated Col-0 and *nia1 nia2* seedlings, suggesting that global metabolic differences have a limited impact on the processes examined here (Fig. 3A,B). In these seedlings, neither ISX-derived reduction of *CYCB1;1* and *CYCD3;1* transcript levels nor increased JA/SA/lignin levels were detectable (Fig. 3A,C,D). Simultaneously, results from the analysis of *nia1 nia2 the1-4* seedlings showed that NIA1 and NIA2 are required to mediate the THE1-dependent responses, implying that NIA1/2-dependent processes are involved in both THE1-dependent and -independent processes (Fig. 3C,D, Fig. S3).

nia1 nia2 seedlings have been used as genetic tool to study NO-based signaling processes and were identified as important regulators of abiotic stress responses (Vicente et al., 2017; Xie et al., 2013). NO has also been suggested to regulate and be regulated by cytokinins, suggesting the existence of a regulatory feedback loop between the two (Tun et al., 2008; Feng et al., 2013; Liu et al., 2013; Shen et al., 2013). In Col-0 seedlings, treated jointly with increasing concentrations of *tZ* and ISX, ISX-induced reductions in *CYCD3;1*

Development (2018) 145, dev166678. doi:10.1242/dev.166678

transcript levels were alleviated in a concentration-dependent manner by *t*Z (Fig. 4A). In *nia1 nia2* seedlings, ISX-induced reductions in transcript levels were absent whereas *tZ* treatment effects were still detectable, implying that the *t*Z-derived effects do not require NIA1 and NIA2 (Fig. 4B). This was supported by results obtained with *ahk3 ahk4* seedlings (Fig. S6E). The results suggested that the effects of ISX on *CYCD3;1* transcript levels and activity might be mediated through changes in cytokinin levels, similar to previously reported regulation of *CYCD3;1* by cytokinins, but may not require histidine kinase-based signaling (Scofield et al., 2013). It remains to be determined whether auxin may also play a role here as previous work has implicated NO-based signaling in stem cell homeostasis through auxin (Sanz et al., 2014).

Cytokinin measurements in ISX-, osmoticum- or ISX/osmoticum-treated Col-0 seedlings showed that individual treatments had opposite effects on certain cytokinins whereas the combined treatments resulted in levels similar to mock controls (Fig. 5). Intriguingly, *i*P-type level changes were particularly similar to *CYCD3;1* transcript level changes, suggesting they may be responsible for changes in transcript levels. Experiments with maize exposed to osmotic stress showed that osmotic stress affects cytokinin levels, but the experimental conditions differed, making comparisons difficult (Vyroubalová et al., 2009). We assessed whether cytokinin signaling is required for the effects of ISX and osmoticum treatments on *CYCD3;1* and *CYCB1;1* transcript levels. In several genotypes (*ahk2 ahk3*, *ahk3 ahk4*, *arr1 arr10 arr12*) we observed lower *CYCD3;1* transcript levels in mock-treated seedlings, corroborating cytokinin function in regulating *CYCD3;1* activity (Scofield et al., 2013) (Fig. S6A-D). *ahk2/3* seedlings exhibited transcript level changes upon treatment with osmoticum only, implicating *AHK2* and *AHK3* in osmoperception, which is in line with their previously described role in drought stress perception (Tran et al., 2007). In all the genotypes examined (also in combination with LGR-991), ISX-induced reductions in transcript levels were still detectable, suggesting that intact cytokinin signaling is not required. However, expression of two genes encoding cytokinin-degrading enzymes (*CKX2*, *CKX3*) was induced by ISX treatment in a *NIA1/2*-dependent and osmosensitive manner. Characterization of *CYCD3;1* and *CYCB1;1* transcript levels in ISX- and/or osmoticum-treated *oeCKX2* and *oeCKX3* seedlings suggested that *CKX2* and *CKX3* overexpression affects ISX- and osmoticum-induced changes (Fig. 6A-C). Bearing in mind that CKX enzymes cleave the isoprenoid side chain of N^6-(Δ^2-isopentenyl) adenine (*i*P), *trans*- and *cis*-zeatin (*t*Z, *c*Z) and their ribosides (iPR, *t*ZR and *c*ZR), leading to adenine/adenosine and the corresponding aldehyde, both CKX2 and CKX3 could be responsible for the observed changes in cytokinin levels (Kopečný et al., 2016). The results suggest that ISX-induced CWD causes increased expression of *CKX2* and *CKX3* through NIA1/2-dependent processes. Increased expression of *CKX2* and *CKX3* could lead to reductions in certain cytokinins, which in turn reduces transcript levels of *CYCD3;1* and cell cycle progression.

We integrated our results with the available information on CWI maintenance signaling into a model summarizing how plant cells respond to ISX-derived CWD (Fig. 7). CWD (generated by ISX or cell wall-degrading enzymes) activates at least three different signaling cascades. One is *THE1*-dependent and responsible for induction of JA/SA/lignin production. A second one activates *PROPEP1* and *PROPEP3* expression, leading to accumulation of PROPEP3 in ISX-treated seedlings (Engelsdorf et al., 2018). These genes encode precursors for signaling peptides enhancing immune responses and attenuating THE1-mediated signaling via

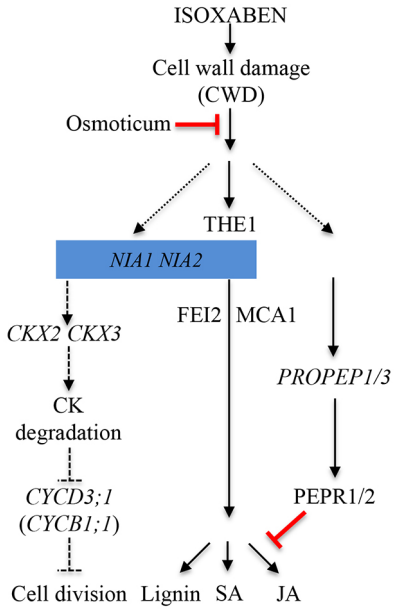

Fig. 7. The mechanism coordinating CWI with cell cycle progression and other ISX-induced responses. ISX-induced CWD responses are osmosensitive. CWD is perceived by at least three signaling pathways: a THE1-dependent pathway, required for induction of JA/SA/lignin production involving also MCA1 and FEI2, and two THE1-independent pathways. The first is responsible for the modulation of CWD-induced JA levels through PROPEP1- and PROPEP3-dependent signaling and requires PEPR1 and PEPR2 (Engelsdorf et al., 2018). The second is responsible for changes in *CYCD3;1* (and *CYCB1;1*) expression, which are similar to alterations observed in the levels of *i*P-type cytokinins. These in turn are correlated with changes in *CKX2* and *CKX3* expression induced by ISX and/or osmoticum treatments. The treatment-induced changes in *CKX2* and *CKX3* transcript levels seem to require *NIA1*- and *NIA2*-dependent processes, which are also required for CWD-induced, *THE1*-dependent SA/JA/lignin production. In this model, *NIA1* and *NIA2*-mediated processes form a hub of the plant CWI maintenance process and could be responsible for changes in levels of *i*P-type cytokinins via controlled degradation, thus modifying *CYCD3;1* activity and possibly leading to changes in cell cycle activity. CK, cytokinin.

their respective receptors PEPR1 and PEPR2 (Bartels and Boller, 2015; Engelsdorf et al., 2018). The third one, also THE1 independent, is responsible for the effects on *CYCD3;1* and *CYCB1;1* transcript levels. *NIA1/2*-dependent processes are required for both *THE1*-dependent and (*THE1*-independent) cell cycle responses, suggesting they form a hub for CWI-related signaling processes. These proteins seem responsible for controlling changes in *CKX2* and *CKX3* transcript levels and thus the cytokinin degradation rate. This is supported by the changes observed in *i*P-type cytokinin levels, which are inversely related to CKX transcript levels. Interestingly, reductions and increases in *i*P-type cytokinins are closely correlated with changes in *CYCD3;1* expression. *CYCD3;1* was identified as a cell cycle regulator, which is active at the G_1/S stage transition (Scofield et al., 2013). Therefore, *CYCD3;1* could act as integrator allowing progression through G_1/S stage only if CWI is intact. This implies the existence of a cell cycle checkpoint in plants, similar to the one described in yeast, dedicated to coordination of CWI and cell cycle activity (Kono et al., 2016).

Our results show that osmoticum reduced many of the ISX-induced responses. Such effects of turgor on cell cycle activity have been observed earlier in plants and yeasts, and have been discussed as important regulators of cell cycle progression (Iraki et al., 1989; Levin and Bartlett-Heubusch, 1992; Sablowski, 2016). We speculate

Development (2018) 145, dev166678. doi:10.1242/dev.166678

that the osmoticum effects occur because CWD involves plasma membrane displacement versus the cell wall, changes in surface tension of the cell wall itself or simply changes in the optimal state of the plasma membrane (stretching/shrinking). These changes could be detected by sensor proteins similar to the mechanisms in place in yeast or animal cells (Austen et al., 2015; Hamant and Haswell, 2017; Heinisch et al., 2010). Elucidation of such sensors will provide the mechanistic insights necessary to understand how CWI is monitored in plants and how downstream responses are activated.

MATERIALS AND METHODS

Plant growth and treatment

Arabidopsis thaliana genotypes used are listed in Table S1. Unless stated otherwise, all results are based on three independent experiments with at least three biological replicates each; all values shown are mean±s.d. Seedlings were sterilized and grown in liquid culture with minor modifications (Hamann et al., 2009). Thirty milligrams of seeds were sterilized by sequential incubation with 70% ethanol and 50% bleach on a rotating mixer for 10 min each and washed three times with sterile water. All experiments were performed in 6-day-old seedlings treated with 600 nM isoxaben (ISX, Sigma-Aldrich; in DMSO), 300 mM sorbitol (s300, Sigma-Aldrich) or a combination of both, in freshly prepared medium. Zeatin (1 mM stock solution) (Sigma-Aldrich) was dissolved in water. Cytokinin competitor LGR-991 was dissolved in DMSO and used at a final concentration of 20 µM. Seedlings were grown in long-day conditions (16 h light, 22°C/8 h dark, 18°C) at 150 µmol m^{-2} s^{-1} photon flux density on a IKA KS501 flask shaker at a constant speed of 130 rotations per minute.

GUS staining

GUS staining was performed using staining buffer containing 50 mm sodium phosphate (pH 7.0), 0.5 mm potassium ferrocyanide, 10 mm EDTA, 0.1% (v/v) Triton X-100, 2% (v/v) dimethyl sulfoxide and 1 mm 5-bromo-4-chloro-3-indolyl-d-glucuronide at 37°C for 24 h (Jefferson et al., 1987; Savatin et al., 2014). Roots and shoots imaged using a Zeiss Axio Zoom-V16 stereomicroscope.

Analysis of root growth phenotypes

Root length measurements were performed right before (0 h) and 24 h after treatments (DMSO/mock, ISX, s300 or ISXs300). Absolute RAM length was determined in primary roots treated for 3, 6 and 9 h. Root tips were stained for 5 min with propidium iodide (1 mg/ml), followed by two washing steps with MilliQ water and imaging using a LSM Zeiss 710 or a Leica SP8. RAM length [defined as the distance between the quiescent center (QC) and the first elongating cell in the root cortical cell layer], RAM size (expressed as number of cortical cells in the RAM), individual cell length and width were measured using Fiji (https://fiji.sc).

Cytokinin measurements

Quantification of cytokinin metabolites was performed according to a method described previously (Svačinová et al., 2012) and slightly modified as described before (Antoniadi et al., 2015). Samples were homogenized and extracted in 1 ml of modified Bieleski buffer (60% methanol, 10% HCOOH and 30% H_2O) together with a cocktail of stable isotope-labeled internal standards (0.25 pmol of cytokinin bases, ribosides, *N*-glucosides and 0.5 pmol of cytokinin *O*-glucosides per sample). Extracts were purified with Oasis MCX column (30 mg/1 ml, Waters) conditioned with 1 ml each of 100% methanol and H_2O, equilibrated sequentially with 1 ml of 50% (v/v) nitric acid, 1 ml of H_2O and 1 ml of 1 M HCOOH. After sample application onto an MCX column, un-retained compounds were removed by a wash step using 1 ml of 1 M HCOOH and 1 ml 100% methanol, pre-concentrated analytes were eluted by two-step elution using 1 ml of 0.35 M NH_4OH aqueous solution and 2 ml of 0.35 M NH_4OH in 60% (v/v) methanol solution. Eluates were evaporated to dryness *in vacuo* and stored at −20°C. Cytokinin levels were determined using ultra-high performance liquid chromatography-electrospray tandem mass spectrometry (UHPLC-MS/MS) (Rittenberg and Foster, 1940).

Salicylic acid and jasmonic acid quantification

JA and SA were analyzed as described by Forcat et al. (2008) with minor modifications as described by Engelsdorf et al. (2018).

Lignin analysis

Lignification was investigated 12 h after start of treatments in root tips. Lignin staining, detection and quantification were performed as described by Engelsdorf et al. (2018).

Quantification of plasma membrane-localized YFP-CesA6 particles

Live cell imaging was performed as described by Ivakov et al. (2017). Col-0 seedlings were grown in flasks containing liquid MS (×0.5), and placed on an orbital shaker (80 rpm; 1.45 ***g***). Six-day-old seedlings were treated with mock (DMSO), 600 nM isoxaben (ISX), 300 mM mannitol (m300) or a combination of isoxaben and mannitol (ISXm300), for 1 h in freshly prepared medium. Seedlings were mounted on a sample holder such that they were sandwiched in between a 1-mm-thick gel pad (1% agarose) and a cover slip. Root epidermal cells in the elongation zone were imaged with a Nikon Ti-E inverted confocal microscope using a CFI APO TIRF 3100 N.A. 1.49 oil immersion objective and evolve CCD camera (Photometrics Technology). Image acquisition was performed with Metamorph software (version 7.5). For plasma membrane CesA6 particle density measurements, an image was acquired at the cell surface, followed by an image at 0.6 µm below the surface in order to image the intracellular CesA6-containing compartments including Golgi and smaCCS/MASCs (small CESA-containing compartments/microtubule-associated CESA compartments). The 'find maxima tool' of ImageJ was used for particle detection within a defined area, using an identical noise threshold.

qRT-PCR

Total RNA was isolated using a Spectrum Plant Total RNA Kit (Sigma-Aldrich). Two micrograms of total RNA were treated with RQ1 RNase-Free DNase (Promega) and cDNA synthesis was performed with the ImProm-II Reverse Transcription System (Promega). qRT-PCR was performed using a LightCycler 480 SYBR Green I Master (Roche) and primers (Table S2) diluted according to manufacturer's specifications. Expression levels of each gene are shown relative to the reference gene *ACT2* and determined using a modified version of the Pfaffl method (Pfaffl et al., 2002) as previously described (Ferrari et al., 2006). LinRegPCR software was used to obtain Cq values and individual PCR efficiency.

Transcriptomic analysis

Total RNA was extracted using a Spectrum Plant Total RNA Kit (Sigma-Aldrich). RNA integrity was assessed using an Agilent RNA 6000 Pico Kit. Sequencing samples were prepared as described previously (Ren et al., 2015). Single-read sequencing was performed for 75 cycles on a NextSeq500 instrument (Illumina RTA v2.4.6). FASTQ files were generated using bcl2fastq2 Conversion Software v1.8.4. Each FASTQ file was subjected to quality control through fastQC v11.1 before technical replicates were combined and an average of 13.1 million reads was produced for each library. Reads were aligned to the *A. thaliana* genome (Ensembl v82) with STAR v2.4.1 in two-pass mode. On average, 96.2% of the reads aligned to the genome. Reads that aligned uniquely to the genome were aggregated into gene counts with Feature Counts v1.4.6 using the genome annotations defined in Ensembl v82. Differentially expressed genes were extracted from Col-0 and *nia1 nia2* genotypes after ISX/mock treatments using DESeq2 differential expression analysis pipeline (Love et al., 2014) in R. For both genotypes, genes showing differential expression in response to ISX treatment versus mock with a 1% false discovery rate (FDR) were considered significantly differentially expressed (DE). In order to assess the variance within the samples, a principal component analysis (PCA) was performed. Regularized logarithm transformation from DESeq2 package was applied to read counts and PCA was performed for 2000 genes with highest variance using a built-in R function 'prcomp'.

The intersection of the DE genes between the genotypes was visualized using a Venn diagram produced with Venny 2.1 (http://bioinfogp.cnb.csic.es/tools/venny/index.html). Analysis of GO categories was performed using AtCOECiS (Vandepoele et al., 2009).

Statistical analysis

Statistical significance (Student's *t*-test, ANOVA) was assessed using IBM SPSS Statistics v24. Statistically significant differences are indicated with different letters for the one-way ANOVA/Tukey's HSD test at α=0.05. Pairwise comparisons, and statistically significant differences according to Student's *t*-test are represented with *P<0.05, **P<0.01, ***P<0.001.

Acknowledgements

The authors thank Hana Martínková and Ivan Petřík for their help with cytokinin analyses and John Mansfield for comments on the manuscript.

Competing interests

The authors declare no competing or financial interests.

Author contributions

Conceptualization: N.G.-B., T.E., L.V., S.P., T.H.; Methodology: N.G.-B., T.E., L.A., T.H.; Validation: N.G.-B., T.E.; Formal analysis: T.E., M.S., L.V., T.H.; Investigation: N.G.-B., T.E., M.S., L.V., G.A.K., A.J., L.A., J.H.; Resources: M.S., L.A., O.N., J.H.; Data curation: L.V.; Writing - original draft: T.H.; Writing - review & editing: N.G.-B., T.E., M.S., L.V., G.A.K., A.J., O.N., S.P., J.H., T.H.; Supervision: T.H.; Project administration: T.H.; Funding acquisition: J.H., T.H.

Funding

This work was supported by a Marie Curie Skłodowska fellowship 'SugarOsmoSignaling' (to T.E.), EEA Grants (7F14155 CYTOWALL to N.G.-B./T.H./J.H.), Ministry of Education, Youth and Sports of the Czech Republic (Ministerstvo Školství, Mládeže a Tělovýchovy) (LQ1601 CEITEC 2020 and LM2015062 Czech-BioImaging) and a European Regional Development Fund Project 'Centre for Experimental Plant Biology' (CZ.02.1.01/0.0/0.0/16_019/0000738).

Data availability

Transcriptomics data have been deposited in Gene Expression Omnibus under accession number GSE109613.

Supplementary information

Supplementary information available online at
http://dev.biologists.org/lookup/doi/10.1242/dev.166678.supplemental

References

Antoniadi, I., Plačková, L., Simonovik, B., Doležal, K., Turnbull, C., Ljung, K. and Novák, O. (2015). Cell-type-specific cytokinin distribution within the arabidopsis primary root apex. *Plant Cell* **27**, 1955-1967.

Austen, K., Ringer, P., Mehlich, A., Chrostek-Grashoff, A., Kluger, C., Klingner, C., Sabass, B., Zent, R., Rief, M. and Grashoff, C. (2015). Extracellular rigidity sensing by talin isoform-specific mechanical linkages. *Nat. Cell Biol.* **17**, 1597-1606.

Bacete, L., Mélida, H., Miedes, E. and Molina, A. (2018). Plant cell wall-mediated immunity: cell wall changes trigger disease resistance responses. *Plant J.* **93**, 614-636.

Bartels, S. and Boller, T. (2015). Quo vadis, Pep? Plant elicitor peptides at the crossroads of immunity, stress, and development. *J. Exp. Bot.* **66**, 5183-5193.

Bartrina, I., Otto, E., Strnad, M., Werner, T. and Schmülling, T. (2011). Cytokinin regulates the activity of reproductive meristems, flower organ size, ovule formation, and thus seed yield in Arabidopsis thaliana. *Plant Cell* **23**, 69-80.

Brenner, W. G., Ramireddy, E., Heyl, A. and Schmülling, T. (2012). Gene Regulation by Cytokinin in Arabidopsis. *Front. Plant Sci.* **3**, 8.

Cano-Delgado, A., Penfield, S., Smith, C., Catley, M. and Bevan, M. (2003). Reduced cellulose synthesis invokes lignification and defense responses in Arabidopsis thaliana. *Plant J.* **34**, 351-362.

Chamizo-Ampudia, A., Sanz-Luque, E., Llamas, A., Galvan, A. and Fernandez, E. (2017). Nitrate reductase regulates plant nitric oxide homeostasis. *Trends Plant Sci.* **22**, 163-174.

Chen, H.-W., Persson, S., Grebe, M. and McFarlane, H. E. (2018). Cellulose synthesis during cell plate assembly. *Physiol. Plant.* **164**, 17-26.

Colón-Carmona, A., You, R., Haimovitch-Gal, T. and Doerner, P. (1999). Spatio-temporal analysis of mitotic activity with a labile cyclin-GUS fusion protein. *Plant J.* **20**, 503-508.

Cosgrove, D. J. (2018). Diffuse growth of plant cell walls. *Plant Physiol.* **176**, 16-27.

Denness, L., McKenna, J. F., Segonzac, C., Wormit, A., Madhou, P., Bennett, M., Mansfield, J., Zipfel, C. and Hamann, T. (2011). Cell wall damage-induced lignin biosynthesis is regulated by a reactive oxygen species- and jasmonic acid-dependent process in Arabidopsis. *Plant Physiol.* **156**, 1364-1374.

Ellis, C. and Turner, J. G. (2001). The Arabidopsis mutant cev1 has constitutively active jasmonate and ethylene signal pathways and enhanced resistance to pathogens. *Plant Cell* **13**, 1025-1033.

Ellis, C., Karafyllidis, I., Wasternack, C. and Turner, J. G. (2002). The Arabidopsis mutant cev1 links cell wall signaling to jasmonate and ethylene responses. *Plant Cell* **14**, 1557-1566.

Engelsdorf, T., Gigli-Bisceglia, N., Veerabagu, M., McKenna, J. F., Vaahtera, L., Augstein, F., Van der Does, D., Zipfel, C. and Hamann, T. (2018). The plant cell wall integrity maintenance and immune signaling systems cooperate to control stress responses in *Arabidopsis thaliana*. *Sci. Signal.* **11**, eaao3070.

Feng, J., Wang, C., Chen, Q., Chen, H., Ren, B., Li, X. and Zuo, J. (2013). S-nitrosylation of phosphotransfer proteins represses cytokinin signaling. *Nat. Commun.* **4**, 1529.

Feng, W., Kita, D., Peaucelle, A., Cartwright, H. N., Doan, V., Duan, Q., Liu, M.-C., Maman, J., Steinhorst, L., Schmitz-Thom, I. et al. (2018). The FERONIA receptor kinase maintains cell-wall integrity during salt stress through Ca 2+ signaling. *Curr. Biol.* **28**, 666-675.e5.

Ferrari, S., Galletti, R., Vairo, D., Cervone, F. and De Lorenzo, G. (2006). Antisense expression of the Arabidopsis thaliana AtPGIP1 gene reduces polygalacturonase-inhibiting protein accumulation and enhances susceptibility to Botrytis cinerea. *Mol. Plant Microbe Interact.* **19**, 931-936.

Forcat, S., Bennett, M. H., Mansfield, J. W. and Grant, M. R. A. (2008). Rapid and robust method for simultaneously measuring changes in the phytohormones ABA, JA and SA in plants following biotic and abiotic stress. *Plant Methods* **4**, 16.

Franck, C. M., Westermann, J. and Boisson-Dernier, A. (2018). Plant malectin-like receptor kinases: from cell wall integrity to immunity and beyond. *Annu. Rev. Plant Biol.* **69**, 301-328.

Furuichi, T., Iida, H., Sokabe, M., Tatsumi, H., Furuichi, T., Iida, H., Sokabe, M. and Tatsumi, H. (2016). Expression of Arabidopsis MCA1 enhanced mechanosensitive channel activity in the Xenopus laevis oocyte plasma membrane Expression of arabidopsis MCA1 enhanced mechanosensitive channel activity in the Xenopus laevis oocyte plasma membrane. *Plant Signal. Behav.* **4**, 1022-1026.

Gigli-Bisceglia, N. and Hamann, T. (2018). Outside-in control - does plant cell wall integrity regulate cell cycle progression? *Physiol. Plant* **164**, 82-94.

Gutierrez, R., Lindeboom, J. J., Paredez, A. R., Emons, A. M. C. and Ehrhardt, D. W. (2009). Arabidopsis cortical microtubules position cellulose synthase delivery to the plasma membrane and interact with cellulose synthase trafficking compartments. *Nat. Cell Biol.* **11**, 797-806.

Hamann, T. (2015). The plant cell wall integrity maintenance mechanism-concepts for organization and mode of action. *Plant Cell Physiol.* **56**, 215-223.

Hamann, T., Bennett, M., Mansfield, J. and Somerville, C. (2009). Identification of cell-wall stress as a hexose-dependent and osmosensitive regulator of plant responses. *Plant J.* **57**, 1015-1026.

Hamant, O. and Haswell, E. S. (2017). Life behind the wall: sensing mechanical cues in plants. *BMC Biol.* **15**, 59.

Haswell, E. S., Peyronnet, R., Barbier-Brygoo, H., Meyerowitz, E. M. and Frachisse, J.-M. (2008). Two MscS homologs provide mechanosensitive channel activities in the Arabidopsis root. *Curr. Biol.* **18**, 730-734.

Heim, D. R., Skomp, J. R., Tschabold, E. E. and Larrinua, I. M. (1990). Isoxaben inhibits the synthesis of acid insoluble cell wall materials in Arabidopsis thaliana. *Plant Physiol.* **93**, 695-700.

Heinisch, J. J., Dupres, V., Alsteens, D. and Dufrêne, Y. F. (2010). Measurement of the mechanical behavior of yeast membrane sensors using single-molecule atomic force microscopy. *Nat. Protoc.* **5**, 670-677.

Hématy, K., Sado, P.-E., Van Tuinen, A., Rochange, S., Desnos, T., Balzergue, S., Pelletier, S., Renou, J.-P. and Höfte, H. (2007). A receptor-like kinase mediates the response of Arabidopsis cells to the inhibition of cellulose synthesis. *Curr. Biol.* **17**, 922-931.

Höfte, H. and Voxeur, A. (2017). Plant cell walls. *Curr. Biol.* **27**, R865-R870.

Honkanen, S., Jones, V. A. S., Morieri, G., Champion, C., Hetherington, A. J., Kelly, S., Proust, H., Saint-Marcoux, D., Prescott, H. and Dolan, L. (2016). The mechanism forming the cell surface of tip-growing rooting cells is conserved among land plants. *Curr. Biol.* **26**, 3238-3244.

Hu, Z., Vanderhaeghen, R., Cools, T., Wang, Y., De Clercq, I., Leroux, O., Nguyen, L., Belt, K., Millar, A. H., Audenaert, D. et al. (2016). Mitochondrial defects confer tolerance against cellulose deficiency. *Plant Cell* **28**, 2010-2017.

Iraki, N. M., Bressan, R. A., Hasegawa, P. M. and Carpita, N. C. (1989). Alteration of the physical and chemical structure of the primary cell wall of growth-limited plant cells adapted to osmotic stress. *Plant Physiol.* **91**, 39-47.

Ivakov, A., Flis, A., Apelt, F., Fünfgeld, M., Scherer, U., Stitt, M., Kragler, F., Vissenberg, K., Persson, S. and Suslov, D. (2017). Cellulose synthesis and cell expansion are regulated by different mechanisms in growing Arabidopsis hypocotyls. *Plant Cell* **29**, 1305-1315.

Jefferson, R. A., Kavanagh, T. A. and Bevan, M. W. (1987). GUS fusions: beta-glucuronidase as a sensitive and versatile gene fusion marker in higher plants. *EMBO J.* **6**, 3901-3907.

Kärkönen, A. and Kuchitsu, K. (2015). Reactive oxygen species in cell wall metabolism and development in plants. *Phytochemistry* **112**, 22-32.

Kohorn, B. D., Kobayashi, M., Johansen, S., Riese, J., Huang, L.-F., Koch, K., Fu, S., Dotson, A. and Byers, N. (2006). An Arabidopsis cell wall-associated kinase required for invertase activity and cell growth. *Plant J.* **46**, 307-316.

Kono, K., Al-Zain, A., Schroeder, L., Nakanishi, M. and Ikui, A. E. (2016). Plasma membrane/cell wall perturbation activates a novel cell cycle checkpoint during G1 in *Saccharomyces cerevisiae*. *Proc. Natl. Acad. Sci. USA* **113**, 6910-6915.

Kopečný, D., Končitíková, R., Popelka, H., Briozzo, P., Vigouroux, A., Kopečná, M., Zalabák, D., Šebela, M., Skopalová J. et al. (2016). Kinetic and structural investigation of the cytokinin oxidase/dehydrogenase active site. *FEBS J.* **283**, 361-377.

Kurusu, T., Nishikawa, D., Yamazaki, Y., Gotoh, M., Nakano, M., Hamada, H., Yamanaka, T., Iida, K., Nakagawa, Y., Saji, H. et al. (2012). Plasma membrane protein OsMCA1 is involved in regulation of hypo-osmotic shock-induced Ca2+ influx and modulates generation of reactive oxygen species in cultured rice cells. *BMC Plant Biol.* **12**, 11.

Levin, D. E. (2011). Regulation of cell wall biogenesis in Saccharomyces cerevisiae: the cell wall integrity signaling pathway. *Genetics* **189**, 1145-1175.

Levin, D. E. and Bartlett-Heubusch, E. (1992). Mutants in the S. cerevisiae PKC1 gene display a cell cycle-specific osmotic stability defect. *J. Cell Biol.* **116**, 1221-1229.

Li, W., Herrera-Estrella, L. and Tran, L.-S. P. (2016). The Yin-Yang of cytokinin homeostasis and drought acclimation/adaptation. *Trends Plant Sci.* **21**, 548-550.

Liu, W.-Z., Kong, D.-D., Gu, X.-X., Gao, H.-B., Wang, J.-Z., Xia, M., Gao, Q., Tian, L.-L., Xu, Z.-H., Bao, F. et al. (2013). Cytokinins can act as suppressors of nitric oxide in Arabidopsis. *Proc. Natl. Acad. Sci. USA* **110**, 1548-1553.

Love, M. I., Huber, W. and Anders, S. (2014). Moderated estimation of fold change and dispersion for RNA-seq data with DESeq2. *Genome Biol.* **15**, 550.

Manfield, I. W., Orfila, C., Mccartney, L., Harholt, J., Bernal, A. J., Scheller, H. V., Gilmartin, P. M., Mikkelsen, J. D., Knox, J. P. and Willats, W. G. T. (2004). Novel cell wall architecture of isoxaben-habituated Arabidopsis suspension-cultured cells: global transcript profiling and cellular analysis. *Plant J.* **40**, 260-275.

McFarlane, H. E., Döring, A. and Persson, S. (2014). The cell biology of cellulose synthesis. *Annu. Rev. Plant Biol.* **65**, 69-94.

Merz, D., Richter, J., Gonneau, M., Sanchez-Rodriguez, C., Eder, T., Sormani, R., Martin, M., Hématy, K., Höfte, H. and Hauser, M.-T. (2017). T-DNA alleles of the receptor kinase THESEUS1 with opposing effects on cell wall integrity signaling. *J. Exp. Bot.* **68**, 4583-4593.

Miart, F., Desprez, T., Biot, E., Morin, H., Belcram, K., Höfte, H., Gonneau, M. and Vernhettes, S. (2014). Spatio-temporal analysis of cellulose synthesis during cell plate formation in Arabidopsis. *Plant J.* **77**, 71-84.

Nakagawa, Y., Katagiri, T., Shinozaki, K., Qi, Z., Tatsumi, H., Furuichi, T., Kishigami, A., Sokabe, M., Kojima, I., Sato, S. et al. (2007). Arabidopsis plasma membrane protein crucial for Ca2+ influx and touch sensing in roots. *Proc. Natl. Acad. Sci. USA* **104**, 3639-3644.

Nguyen, K. H., Van Ha, C., Nishiyama, R., Watanabe, Y., Leyva-González, M. A., Fujita, Y., Tran, U. T., Li, W., Tanaka, M., Seki, M. et al. (2016). *Arabidopsis* type B cytokinin response regulators ARR1, ARR10, and ARR12 negatively regulate plant responses to drought. *Proc. Natl. Acad. Sci. USA* **113**, 3090-3095.

Nicol, F. and Höfte, H. (1998). Plant cell expansion: scaling the wall. *Curr. Opin. Plant Biol.* **1**, 12-17.

Nishiyama, R., Watanabe, Y., Fujita, Y., Le, D. T., Kojima, M., Werner, T., Vankova, R., Yamaguchi-Shinozaki, K., Shinozaki, K., Kakimoto, T. et al. (2012). Analysis of cytokinin mutants and regulation of cytokinin metabolic genes reveals important regulatory roles of cytokinins in drought, salt and abscisic Acid responses, and abscisic Acid biosynthesis. *Plant Cell* **23**, 2169-2183.

Nisler, J., Zatloukal, M., Popa, I., Doležal, K., Strnad, M. and Spíchal, L. (2010). Cytokinin receptor antagonists derived from 6-benzylaminopurine. *Phytochemistry* **71**, 823-830.

Okushima, Y., Shimizu, K., Ishida, T., Sugimoto, K. and Umeda, M. (2014). Differential regulation of B2-type CDK accumulation in Arabidopsis roots. *Plant Cell Rep.* **33**, 1033-1040.

Paidhungat, M. and Garrett, S. (1997). A homolog of mammalian, voltage-gated calcium channels mediates yeast pheromone-stimulated Ca2+ uptake and exacerbates the cdc1(Ts) growth defect. *Mol. Cell. Biol.* **17**, 6339-6347.

Paniagua, C., Bilkova, A., Jackson, P., Dabravolski, S., Riber, W., Didi, V., Houser, J., Gigli-Bisceglia, N., Wimmerova, M., Budínská, E. et al. (2017). Dirigent proteins in plants: modulating cell wall metabolism during abiotic and biotic stress exposure. *J. Exp. Bot.* **68**, 3287-3301.

Paredez, A. R., Somerville, C. R. and Ehrhardt, D. W. (2006). Visualization of cellulose synthase demonstrates functional association with microtubules. *Science* **312**, 1491-1495.

Pfaffl, M. W., Horgan, G. W. and Dempfle, L. (2002). Relative expression software tool (REST (C)) for group-wise comparison and statistical analysis of relative expression results in real-time PCR. *Nucleic Acids Res.* **30**, e36.

Polyn, S., Willems, A. and De Veylder, L. (2015). Cell cycle entry, maintenance, and exit during plant development. *Curr. Opin. Plant Biol.* **23**, 1-7.

Ren, N., Gao, G., Sun, Y., Zhang, L., Wang, H., Hua, W., Wan, K. and Li, X. (2015). MicroRNA signatures from multidrug-resistant Mycobacterium tuberculosis. *Mol. Med. Rep.* **12**, 6561-6567.

Riou-Khamlichi, C., Menges, M., Healy, J. M. S. and Murray, J. A. H. (2000). Sugar control of the plant cell cycle: differential regulation of Arabidopsis D-type cyclin gene expression. *Mol. Cell. Biol.* **20**, 4513-4521.

Rittenberg, D. and Foster, L. (1940). A new procedure for quantitative analysis by isotope dilution, with application to the determination of amino acids and fatty acids. *J. Biol. Chem.* **133**, 727-744.

Rosa, M., Abraham-Juárez, M. J., Lewis, M. W., Fonseca, J. P., Tian, W., Ramirez, V., Luan, S., Pauly, M. and Hake, S. (2017). The Maize MID-COMPLEMENTING ACTIVITY Homolog CELL NUMBER REGULATOR13/NARROW ODD DWARF Coordinates Organ Growth and Tissue Patterning. *Plant Cell* **29**, 474-490.

Sablowski, R. (2016). Coordination of plant cell growth and division: collective control or mutual agreement? *Curr. Opin. Plant Biol.* **34**, 54-60.

Sanz, L., Fernandez-Marcos, M., Modrego, A., Lewis, D. R., Muday, G. K., Pollmann, S., Duenas, M., Santos-Buelga, C. and Lorenzo, O. (2014). Nitric oxide plays a role in stem cell niche homeostasis through its interaction with Auxin. *Plant Physiol.* **166**, 1972-1984.

Savatin, D. V., Bisceglia, N. G., Marti, L., Fabbri, C., Cervone, F. and De Lorenzo, G. (2014). The Arabidopsis NPK1-related protein kinases ANPs are required for elicitor-induced oxidative burst and immunity. *Plant Physiol.* **165**, 1188-1202.

Schaller, G. E., Street, I. H. and Kieber, J. J. (2014). Cytokinin and the cell cycle. *Curr. Opin. Plant Biol.* **21**, 7-15.

Scheible, W.-R., Eshed, R., Richmond, T., Delmer, D. and Somerville, C. (2001). Modifications of cellulose synthase confer resistance to isoxaben and thiazolidinone herbicides in Arabidopsis Ixr1 mutants. *Proc. Natl. Acad. Sci. USA* **98**, 10079-10084.

Scofield, S., Dewitte, W., Nieuwland, J. and Murray, J. A. H. (2013). The Arabidopsis homeobox gene *SHOOT MERISTEMLESS* has cellular and meristem-organisational roles with differential requirements for cytokinin and CYCD3 activity. *Plant J.* **75**, 53-66.

Shen, Q., Wang, Y.-T., Tian, H. and Guo, F.-Q. (2013). Nitric oxide mediates cytokinin functions in cell proliferation and meristem maintenance in arabidopsis. *Mol. Plant* **6**, 1214-1225.

Skirycz, A., Claeys, H., De Bodt, S., Oikawa, A., Shinoda, S., Andriankaja, M., Maleux, K., Eloy, N. B., Coppens, F., Yoo, S.-D. et al. (2011). Pause-and-stop: the effects of osmotic stress on cell proliferation during early leaf development in *Arabidopsis* and a role for ethylene signaling in cell cycle arrest. *Plant Cell* **23**, 1876-1888.

Svačinová, J., Novák, O., Plačková, L., Lenobel, R., Holík, J., Strnad, M. and Doležal, K. (2012). A new approach for cytokinin isolation from Arabidopsis tissues using miniaturized purification: pipette tip solid-phase extraction. *Plant Methods* **8**, 17.

Świątek, A., Azmi, A., Stals, H., Inze, D. and Van Onckelen, H. (2004). Jasmonic acid prevents the accumulation of cyclin B1;1 and CDK-B in synchronized tobacco BY-2 cells. *FEBS Lett* **572**, 118-122.

Tateno, M., Brabham, C. and DeBolt, S. (2016). Cellulose biosynthesis inhibitors - a multifunctional toolbox. *J. Exp. Bot.* **67**, 533-542.

Tenhaken, R. (2014). Cell wall remodeling under abiotic stress. *Front. Plant Sci.* **5**, 771.

Tran, L.-S. P., Urao, T., Qin, F., Maruyama, K., Kakimoto, T., Shinozaki, K. and Yamaguchi-Shinozaki, K. (2007). Functional analysis of AHK1/ATHK1 and cytokinin receptor histidine kinases in response to abscisic acid, drought, and salt stress in Arabidopsis. *Proc. Natl. Acad. Sci. USA* **104**, 20623-20628.

Tsang, D. L., Edmond, C., Harrington, J. L. and Nuhse, T. S. (2011). Cell wall integrity controls root elongation via a general 1-aminocyclopropane-1-carboxylic acid-dependent, ethylene-independent pathway. *Plant Physiol.* **156**, 596-604.

Tun, N. N., Livaja, M., Kieber, J. J. and Scherer, G. F. E. (2008). Zeatin-induced nitric oxide (NO) biosynthesis in Arabidopsis thaliana mutants of NO biosynthesis and of two-component signaling genes. *New Phytol.* **178**, 515-531.

Van der Does, D., Boutrot, F., Engelsdorf, T., Rhodes, J., McKenna, J. F., Vernhettes, S., Koevoets, I., Tintor, N., Veerabagu, M., Miedes, E. et al. (2017). The Arabidopsis leucine-rich repeat receptor kinase MIK2/LRR-KISS connects cell wall integrity sensing, root growth and response to abiotic and biotic stresses. *PLoS Genet.* **13**, e1006832.

Vandepoele, K., Quimbaya, M., Casneuf, T., De Veylder, L. and Van de Peer, Y. (2009). Unraveling Transcriptional Control in Arabidopsis Using cis-Regulatory Elements and Coexpression Networks. *Plant Physiol.* **150**, 535-546.

Vicente, J., Mendiondo, G. M., Movahedi, M., Charng, Y.-Y., Gray, J. E., Holdsworth Correspondence, M. J., Peirats-Llobet, M., Juan, Y.-T., Shen, Y.-Y., Dambire, C. et al. (2017). The Cys-Arg/N-end rule pathway is a general sensor of abiotic stress in flowering plants. *Curr. Biol.* **27**, 3183-3190.e4.

Vyroubalová, S., Václavíková, K., Turecková, V., Novák, O., Smehilová, M., Hluska, T., Ohnoutková, L., Frébort, I. and Galuszka, P. (2009). Characterization of new maize genes putatively involved in cytokinin metabolism and their expression during osmotic stress in relation to cytokinin levels. *Plant Physiol.* **151**, 433-447.

Watanabe, Y., Schneider, R., Barkwill, S., Gonzales-Vigil, E., Hill, J. L., Samuels, A. L., Persson, S. and Mansfield, S. D. (2018). Cellulose synthase complexes display distinct dynamic behaviors during xylem transdifferentiation. *Proc. Natl. Acad. Sci. USA* **115**, E6366-E6374.

Werner, T., Motyka, V., Laucou, V., Smets, R., Van Onckelen, H. and Schmülling, T. (2003). Cytokinin-deficient transgenic arabidopsis plants show multiple developmental alterations indicating opposite functions of cytokinins in the regulation of shoot and root meristem activity. *Plant Cell* **15**, 2532-2550.

Wilson, M. E., Mixdorf, M., Berg, R. H. and Haswell, E. S. (2016). Plastid osmotic stress influences cell differentiation at the plant shoot apex. *Development* **143**, 3382-3393.

Wolf, S. (2017). Plant cell wall signalling and receptor-like kinases. *Biochem. J.* **474**, 471-492.

Wormit, A., Butt, S. M., Chairam, I., McKenna, J. F., Nunes-Nesi, A., Kjaer, L., O'Donnelly, K., Fernie, A. R., Woscholski, R., Barter, M. C. L. et al. (2012). Osmosensitive changes of carbohydrate metabolism in response to cellulose biosynthesis inhibition. *Plant Physiol.* **159**, 105-117.

Xie, Y., Mao, Y., Lai, D., Zhang, W., Zheng, T. and Shen, W. (2013). Roles of NIA/NR/NOA1-dependent nitric oxide production and HY1 expression in the modulation of Arabidopsis salt tolerance. *J. Exp. Bot.* **64**, 3045-3060.

Xu, S.-L., Rahman, A., Baskin, T. I. and Kieber, J. J. (2008). Two leucine-rich repeat receptor kinases mediate signaling, linking cell wall biosynthesis and ACC synthase in Arabidopsis. *Plant Cell* **20**, 3065-3079.

Yamanaka, T., Nakagawa, Y., Mori, K., Nakano, M., Imamura, T., Kataoka, H., Terashima, A., Iida, K., Kojima, I., Katagiri, T. et al. (2010). MCA1 and MCA2 that mediate Ca2+ uptake have distinct and overlapping roles in Arabidopsis. *Plant Physiol.* **152**, 1284-1296.

Zhao, Q. and Dixon, R. A. (2014). Altering the cell wall and its impact on plant disease: from forage to bioenergy. *Annu. Rev. Phytopathol.* **52**, 69-91.

Zhao, L., Li, Y., Xie, Q. and Wu, Y. (2017). Loss of CDKC;2 increases both cell division and drought tolerance in Arabidopsis thaliana. *Plant J.* **91**, 816-828.

Zürcher, E. and Müller, B. (2016). Cytokinin synthesis, signaling, and function – Advances and new insights. *Int. Rev. Cell. Mol. Biol.* **324**, 1-38.